# 10

# EXAMPLES OF CLINICAL APPLICATIONS OF BIOEFFECT PLANNING

In the preceding chapters fundamental radiobiological principles have been explored, models that may be used for bioeffect planning have been written, and appropriate normal tissue, tumor, and treatment variables have been described and quantified. An important component of the book so far has also been to test the models and plausible parameter values against clinical results. Finally, in this chapter and the appendixes, examples of bioeffect plans applied to clinical circumstances and patients are presented.

Attention has been drawn to impediments to the development of bioeffect planning, some of which are as follows:

- There is justifiable concern about the accuracy of tumor and normal tissue parameter values and radiobiological models in general, as Box (1984) aptly stated “all models are wrong” but added “but some are useful.” Much of this monograph has been directed to describing the usefulness of the models derived.
- There is a comparative lack of appreciation by clinicians of the disparities of predictions of biological effect as judged from isodose plans and the effects predicted with bioeffect plans in many common clinical circumstances. The use of dose per fraction contours (rad displays) combined with look-up graphs developed in this book, some of which are shown in earlier chapters, is the simplest way for clinicians to appreciate the differences between isodose and bioeffect planning and understand how misleading isodose planning sometimes may be. The fundamental deficiency of isodose planning is that the biological effect is usually not directly proportional to dose but is usually related to dose in complex and subtle ways with differing “Shades of Gray.”
- Clinicians are often not comfortable with what are frequently quite complicated mathematical models. The demonstration of relevant interactive biological models and equations derived throughout this book that may also be displayed through a data-show tablet is a simple means for clinicians to become familiar with a wide range of models and their sensitivity to changes in the variables.

- Commercial radiotherapy planning systems have not been available to develop useful bioeffect plans. The development of the Adelaide Bioeffect Planning System now provides a means of fully interactive bioeffect planning for both fractionated and continuous irradiation using a conventional radiotherapy computer planning system. By this means direct comparisons can be made with standard isodose plans. The system is capable of being programmed with any models of interest of which only a few examples are shown in this chapter and the Appendixes.

*The main conclusion of this work is that it is time for bioeffect planning systems such as the Adelaide Bioeffect Planning System to be developed elsewhere to be used as an experimental tool to compare bioeffect plans with conventional isodose plans and to explore the potential for clinical applications of relevant radiobiological models using "plausible" tumor and normal tissue parameter values.*

## 10.1 Introduction

So far in this work attention has been directed to basic radiobiological theory, the development of appropriate radiobiological models, and definition of normal tissue, tumor, and treatment parameter values that may be used in appropriate models. Special emphasis has been placed on applying the models to clinical protocols to check their predictive value.

The need for bioeffect planning has been apparent to the author for many years and the first paper published by the author on the deficiencies of isodose planning was Wigg and Wilson (1981), which is included herein as Appendix C. In this the serious consequences of treating one field per day in a parallel pair technique are demonstrated. That paper was written to demonstrate the need to treat all fields daily to reduce the high incidence of radiation enteritis occurring then in South Australia as a consequence of this technique (Kwitko et al. 1982). At that time the only radiobiological model with clinically derived parameters available for gut tolerance was the cell population kinetic (CPK) model of Cohen described in chapter 1, Early Models of Clinical Importance "Wrong but Useful Models," and for this reason it was the first applied using the Adelaide Bioeffect Program to the examination of clinical cases, examples of which are shown in section 10.5.1. Because of the relatively long history of the development of the Adelaide Bioeffect Planning System older models were initially used and for completeness of this monograph some examples are shown in this section. Examples are shown where isodose planning is clearly misleading, as can be demonstrated with bioeffect planning. While it is acknowledged frequently in this book that there are inherent uncertainties and potential hazards using predictive models in bioeffect planning, these hazards must be judged against the potential deficiencies of isodose planning. It is for this reason that it is argued that bioeffect plans must always be compared with

the gold standard of isodose plans. It is argued that the development of commercial computer planning systems with the option of simultaneous display of experimental bioeffect and isodose plans is necessary before the deficiencies of conventional isodose plans will be widely appreciated.

Examples of the first bioeffect plans generated by Nicholls and Wigg in 1983 are shown in figure 10.1. These figures were presented by Nicholls at the Engineering and Physics in the Life Sciences Conference in Sydney in 1983. Figure 10.1 shows lung corrected plans for stromal tissue and spinal cord in which bioeffect contours are plotted. The treatment techniques, models, program operation, and design criteria of the system are described in Appendixes A and B, which report on some of the early bioeffect plans generated to demonstrate disparities between biological effect predicted by bioeffect plans and isodose plans.

Since these early developments the IGE Target Planning System has been programmed with a variety of newer models developed by the author and described in this work. These include models for fractionated irradiation alone or combined with continuous irradiation, continuous irradiation alone, and tumor control probability models. Work is also in progress by the author and the staff of the Department of Medical Physics, Royal Adelaide Hospital to incorporate bioeffect planning into the Fischer–Leibinger Stereotactic Planning System (Howmedica Leiginger GmbH and Co. KG Pfizer Medical Technology Group, Freiburg, Germany). Appropriate models derived by the author for stereotactic treatment have been described in chapter 7, A Radiobiological Basis for the Treatment of Arteriovenous Malformations.

## 10.2 Impediments to the Development of Bioeffect Planning

As far as is known the Adelaide Bioeffect Planning System has been the only one of its type since 1983, and only very recently some interest has been shown by current manufacturers of planning systems. There are several reasons why so little interest has been taken in bioeffect planning, especially at the level of developing suitable computers for clinical use.

- The culture of isodose planning is deeply imbedded in the history of radiotherapy planning which evolved from manual planning and continued with early and current computer planning systems. Radiation oncologists have for decades become accustomed to isodose

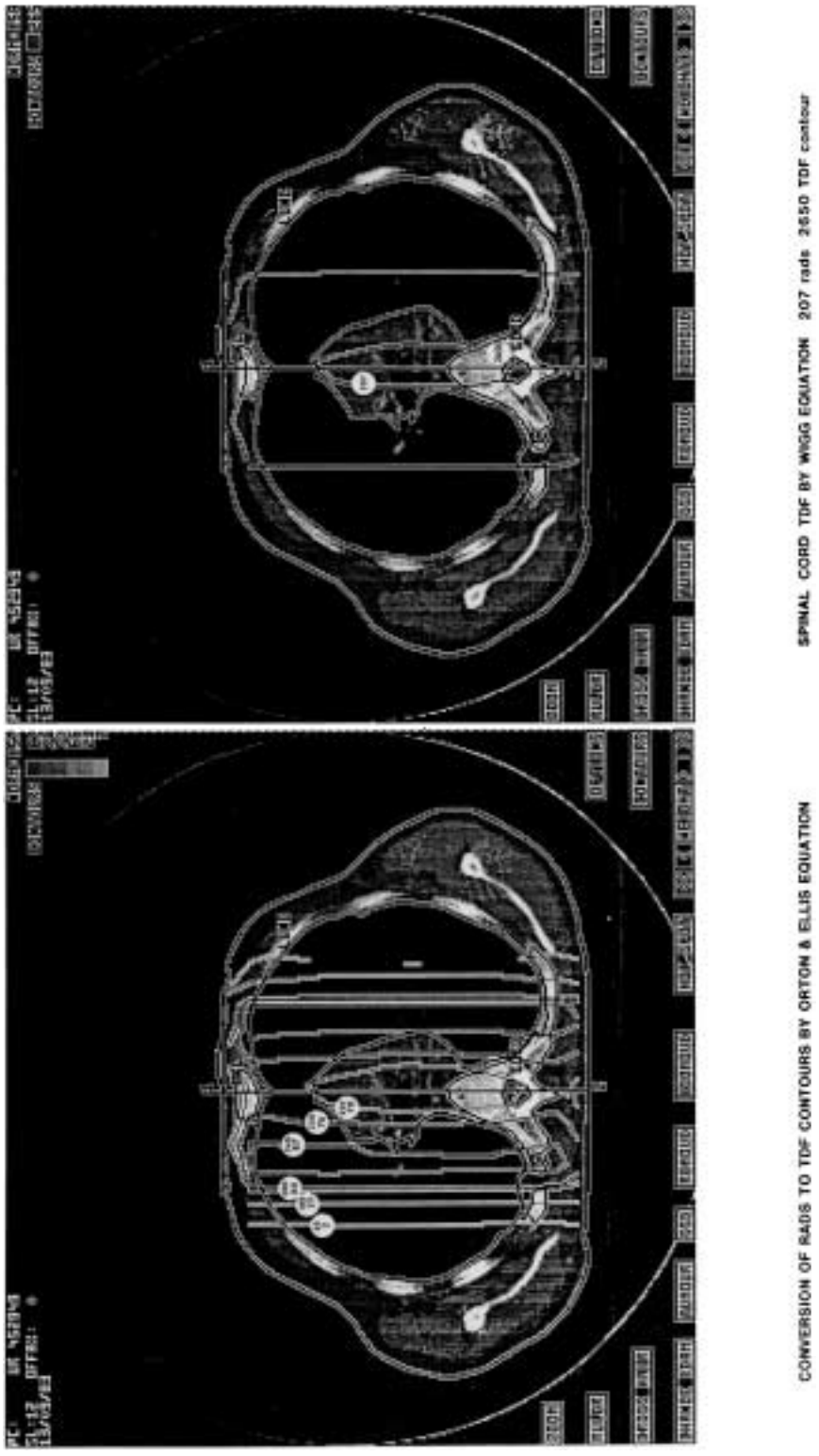


**Figure 10.1** The first Adelaide Bioeffect Plans.

planning, and the large body of accumulated experience with isodose planning remains the benchmark for treatment.

- There is considerable justifiable concern about the use of radiobiological models to predict clinical effects. Radiotherapy history is littered with disasters resulting from the misapplication of models or the use of models of dubious value.
- Models are frequently published in a form not readily applicable to bioeffect planning, an issue which has been addressed in this book.
- It is only fairly recently that models have been developed that are appearing to be of reasonably reliable predictive value, especially for late effects.
- There is considerable uncertainty regarding "plausible" parameter values that may be used. This issue has been addressed particularly in chapter 8, Plausible Parameter Values of Normal and Tumor that May be Used for Predictive Models and Bioeffect Planning.
- The nonavailability of computer planning systems capable of generating bioeffect plans for comparison with isodose plans.
- Fear of litigation both by manufacturers and potential users of nonconventional systems. This must be judged against potential litigation using inappropriate isodose plans.
- Many radiation oncologists are not comfortable with the mathematics required, whereas physicists are, but may not necessarily fully appreciate the biological implications.

At one level radiation oncologists nowadays are aware of the many variables that determine tissue effects; for example, the importance of dose per fraction. At another level the effects of variation of dose per fraction in a 3-D target volume present problems and these effects are not intuitively apparent. For this reason the first, simplest, and probably the most important step is to generate dose per fraction plots (rad displays). The term "rad display" used here as scaling of the dose per fraction displays in the target planning system in use is such that the dose per fraction is most conveniently described in centiGray or rad. Biologically effective doses, for example, for late effects may be simply derived with the use of look-up graphs as presented in chapter 1.

Familiarity with the biological significance of mathematical models can be assisted by "seeing," with live presentations, the effects of changes of variables. For this reason an important part of this monograph has been to develop a means of demonstrating useful models for teaching purposes in a "live" interactive form on a computer and by generating

full bioeffect plans which may be viewed on the radiotherapy computer console or as hard copies. Examples of bioeffect plans are presented below.

## 10.3 A Teaching Tool: Display of "Live" Interactive Models

An important part of this work has been the development of appropriate models which may be displayed as interactive graphs on a computer in which the variables may be changed and the effects instantly seen. Examples of such models, which are particularly useful for teaching purposes, are the models EFFECT, OPTIMUM, and CONFRACT, but almost all graphs shown in this work are interactive and can also be used in the same way.

Figure 10.2 shows the use of a laptop computer from which the EFFECT model is displayed through a data-show tablet. This method has been in routine use for teaching and presentation purposes and is a simple way to demonstrate the biological significance of mathematical models and the parameters used.

## 10.4 The First Step to Bioeffect Planning in the Clinic: Dose Per Fraction Display Plots

Figure 10.3 is a simple example of displaying the contours in dose per fraction rather than % dose. With the target planning system the scale is necessarily displayed in rad (cGy). In this figure, a 10-MV parallel pair of $8 \times 10$ cm fields at 100 cm SAD are used to treat a mediastinal mass using a relative density lung correction of 0.25. Although 200 cGy per fraction is prescribed to mid separation, the spinal cord receives 210 cGy, and clearly cord tolerance is dose limiting. Appropriate look-up charts, as discussed in chapter 1, may be used to determine cord tolerance which, by interpolating from figure 1.10, $22 \times 2.10$, is equivalent to $24 \times 2.0$ Gy and which, if accepted as a tolerance dose, indicates the limit for this phase of treatment. The "hot spot" is 220 cGy and if stroma of $\alpha/\beta$ = 3.0 Gy is of interest the biologically effective dose of $22 \times 220$ cGy from the look-up graph, figure 1.3 is the equivalent of $25 \times 2.0$ Gy. If the biologically effective dose at a given point within the lung is of interest, this may be derived using an appropriate look-up graph for lung. The use of appropriate look-up graphs for tissues of interest may simply be applied to any "rad display" treatment plan in the clinic. This method has been routinely used by the author for many years. A family of look-up graphs have been prepared, a few of which are shown in chapter 1.

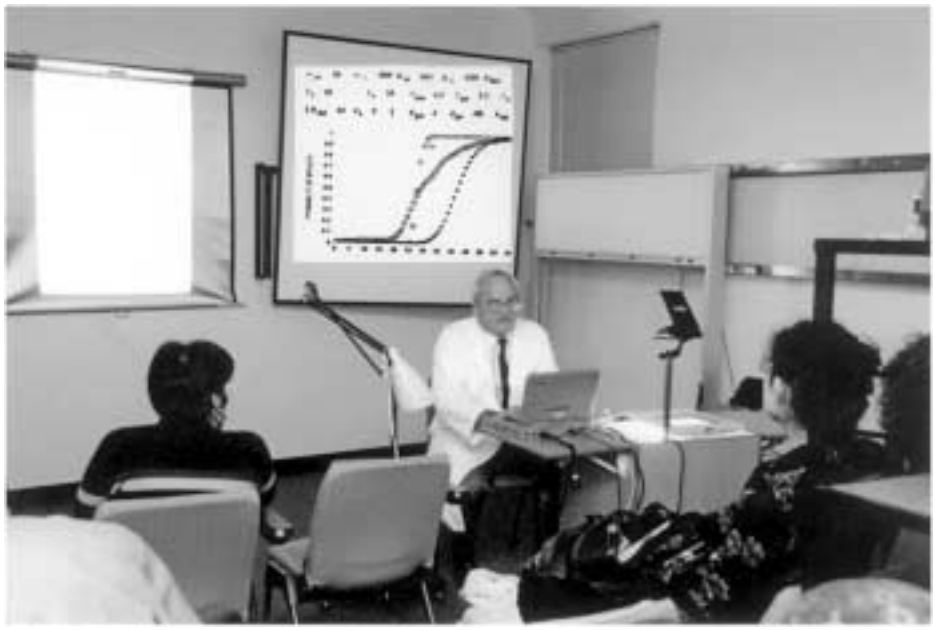

**Figure 10.2** The use of interactive "live" graphs to demonstrate the biological implications of appropriate models and the effect of changes in parameter values.The model displayed is the EFFECT model. It is difficult to "see" the interaction between the variables and their sensitivities when juggling many variables. Models such as the EFFECT model are means of simplifying the process.

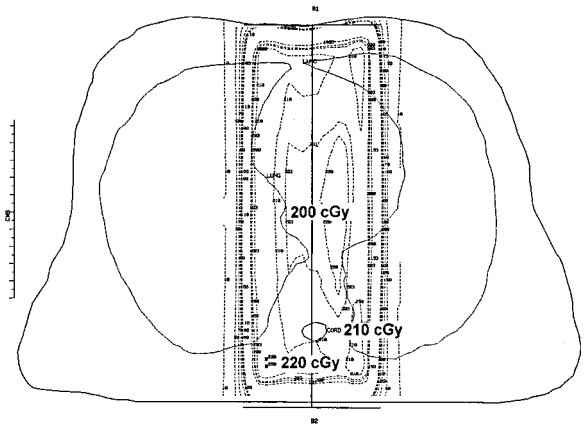


**Figure 10.3** Dose display (rad display) in cGy per fraction. From this the biologically effective dose in tissues and points of interest may be derived in the clinic using appropriate look-up graphs.

## 10.5 Examples of Bioeffect Plans

### 10.5.1 CPK Multi-Target Model Applied to Cases of Radiation Enteritis

The earliest clinical application of the bioeffect planning system was the examination of a local problem of radiation enteritis. The CPK model was used for bioeffect planning because at that time there was no other available for late radiation enteropathy and for which parameter values from clinical data were available. The parameter values and the models described by Cohen and Creditor (1983) were derived from analysis of all clinical data available to them at that time.

The Cohen CPK multi-target model described in section 1.4 has been used to examine a series of patients with radiation enteritis treated at the Royal Adelaide Hospital (Kwitko et al. 1982). All patients were treated with one field per day (a practice now discontinued) and no chemotherapy was used. As CT was not available during the period these patients were treated (1974–1979), a representative CT was used, the peritoneal cavity was outlined, and the CT contours were altered to match the individual patient's separation.

The design of the bioeffect planning system is described in Appendixes A–C. "Look-up" tables as described by Nicholls and Wigg (1984) may be generated for the model being used and the number of fractions being treated. Figure 10.4 is an example of such a "look-up" table for the CPK multi-target model for gut treating for 17 fractions. The table consists of columns of dose per fraction in the tissues and the corresponding $Q$

LOOK-UP TABLE GENERATED BY L.COHEN'S CELKIL(VERSION 1)

MULTI-TARGET MODEL

RADIATION ENTEROPATHY

1.64 MEAN CELLULAR LETHAL DOSE, D.Ø
2Ø. EXTRAPOLATION NUMBER
Ø.1Ø INITIAL REGENERATION RATE, L
2.4Ø RATIO K/J, OR (SQRT BETA)/ALPHA, RHO
17.ØØ LIMIT NO. REPOPULATION CELL CYCLES, G
Ø.22 FIELD SIZE, OR TUMOUR VOL.DEP. FACTOR, Y
2.2Ø AVERAGE INTERVAL BETWEEN FRACTIONS, V
14.ØØ FIELD OR TUMOUR SIZE, Z
17 NUMBER OF FRACTIONS, N

| DOSE/FR. | Q | DOSE/FR. | Q | DOSE/FR. | Q | DOSE/FR. | Q | DOSE/FR. | Q |
|---|---|---|---|---|---|---|---|---|---|
| 15Ø | 1.Ø6 | 151 | 1.Ø7 | 152 | 1.Ø8 | 153 | 1.Ø9 | 154 | 1.11 |
| 155 | 1.12 | 156 | 1.13 | 157 | 1.14 | 158 | 1.15 | 159 | 1.16 |
| 16Ø | 1.17 | 161 | 1.18 | 162 | 1.19 | 163 | 1.2Ø | 164 | 1.21 |
| 165 | 1.22 | 166 | 1.23 | 167 | 1.25 | 168 | 1.26 | 169 | 1.27 |
| 17Ø | 1.28 | 171 | 1.29 | 172 | 1.3Ø | 173 | 1.31 | 174 | 1.32 |
| 175 | 1.34 | 176 | 1.35 | 177 | 1.36 | 178 | 1.37 | 179 | 1.38 |
| 18Ø | 1.39 | 181 | 1.4Ø | 182 | 1.42 | 183 | 1.43 | 184 | 1.44 |
| 185 | 1.45 | 186 | 1.46 | 187 | 1.47 | 188 | 1.49 | 189 | 1.5Ø |
| 19Ø | 1.51 | 191 | 1.52 | 192 | 1.53 | 193 | 1.54 | 194 | 1.56 |
| 195 | 1.57 | 196 | 1.58 | 197 | 1.59 | 198 | 1.6Ø | 199 | 1.62 |
| 2ØØ | 1.63 | 2Ø1 | 1.64 | 2Ø2 | 1.65 | 2Ø3 | 1.66 | 2Ø4 | 1.68 |

**Figure 10.4** A portion of a "look-up" table for radiation enteropathy using the Cohen CELL KILL multi-target model. The parameter values used for 17 fractions are shown above the table. The dose per fraction varies from 1.50 cGy to 204 cGy and the corresponding *Q* values (multiplied × 10) vary from 1.08 to 1.68.

values (×10) of the CPK model, and the parameter values are shown above the table.

Figures 10.5–10.13 are bioeffect plans of patients each of which developed late radiation enteropathy as predicted by the CPK model, even though the treatment parameters were quite variable and each was treated with one field only per day. In each figure the contours are in units of *Q* (×10) from which the percent risk of radiation enteritis has been derived by calculating the Probit value from the *Q* values, as described previously in chapter 1. Probit transformation tables were used to transform the Probit values to percent risk of radiation enteropathy and shown as the tissue complication probability in figures 10.5–10.13.

Figure 10.14 shows that all the cases shown in figures 10.5–10.13 had a predicted significant risk of radiation enteritis. Although the shortcomings of the CPK model have been described in chapter 1, it is of interest that this model was useful in demonstrating the ill effects of treating one field per day.

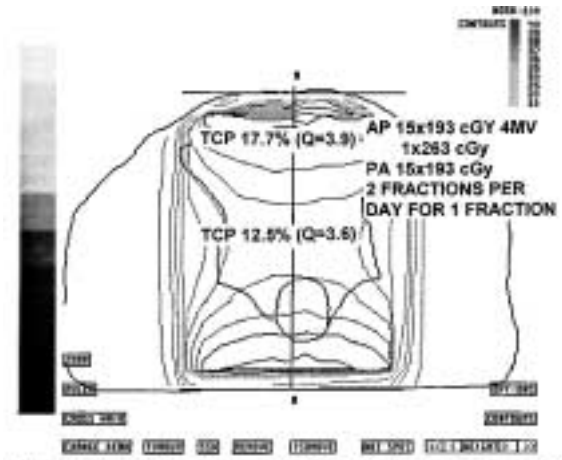


**Figure 10.5** Patient W.U. dose at center 5750 cGy, in 43 days, 4 MV, sep. 20 cm, equiv. sq 16.5 cm.

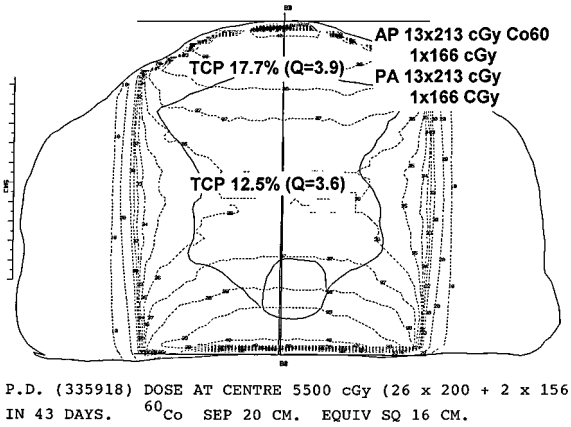


**Figure 10.6** Patient P.D. dose at center 5500 cGy, in 43 days, $^{60}$Co, sep. 20 cm, equiv. sq. 16 cm.

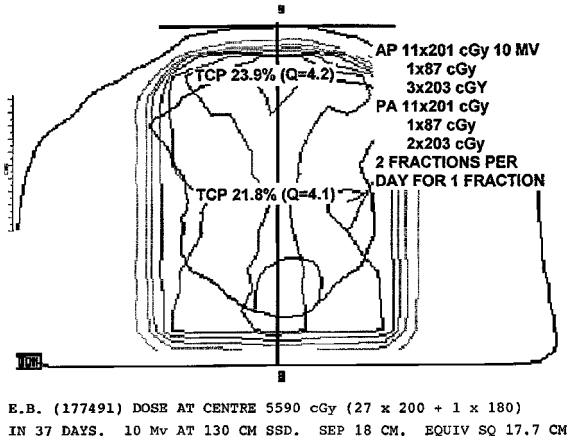


**Figure 10.7** Patient E.B. dose at center 5590 cGy, in 37 days, 10 MV, ssd = 130 cm, sep. 18 cm, equiv. sq. 17.7 cm.

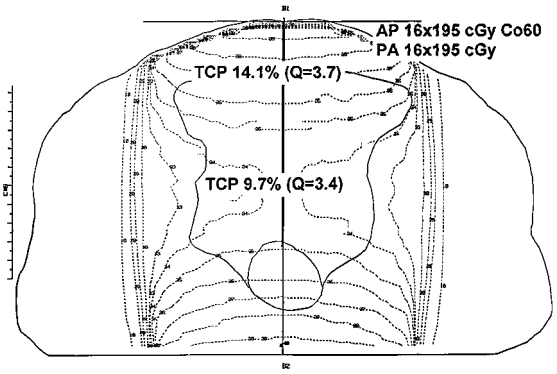


P.G. (188641) DOSE AT CENTRE 5750 cGy (32 x 180) IN 44 DAYS.
$^{60}$Co. SEP 18 CM. EQUIV SQ 14.2 CM.

**Figure 10.8** Patient P.G. dose at center 5750 cGy, in 44 days, $^{60}$Co, ssd = 75 cm, sep. 18 cm, equiv. sq. 14.2 cm.

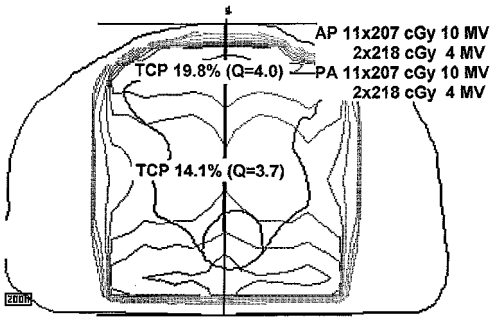


M.G. (35537) DOSE AT CENTRE 5190 cGy (26 x 200) IN 39 DAYS.
10 Mv AND 4 Mv. SEP 23 CM. EQUIV SQ 20.5 CM

**Figure 10.9** Patient M.G. dose at center 5190 cGy, in 39 days, 10 MV and 4 MV, ssd = 100 cm, sep. 23 cm, equiv. sq. 20.5 cm.

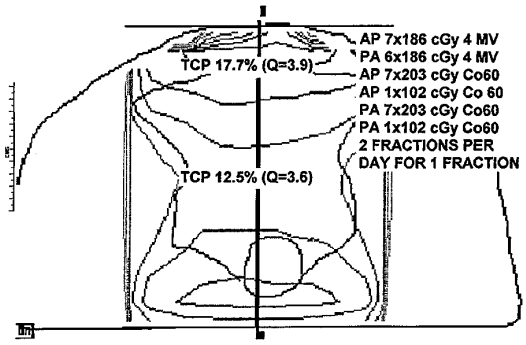


J.McB (38162) DOSE AT CENTRE 5277 cGy (13 x 183 + 15 x 193)
IN 48 DAYS. 4 Mv AND $^{60}$Co. SEP 17 CM. EQUIV SQ 14.8 CM.

**Figure 10.10** Patient J.McB. dose at center 5277 cGy, in 48 days, 4 MV and $^{60}$Co, ssd = 100 and 75 cm, sep. 17 cm, equiv. sq. 14.8 cm.

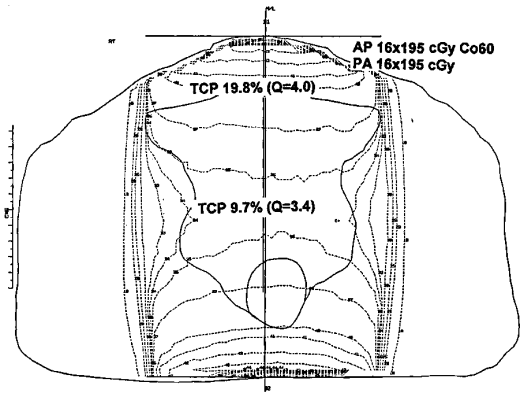


**Figure 10.11** Patient C.A. dose at center 5500 cGy, in 43 days, $^{60}$Co, ssd = 75 cm, sep. 22 cm, equiv. sq. 16.5 cm.

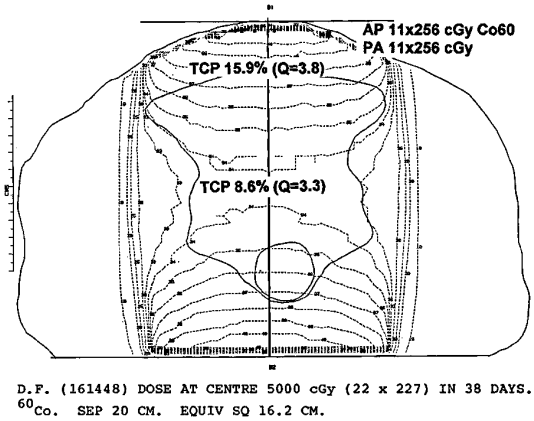


**Figure 10.12** Patient D.F. dose at center 5000 cGy, in 38 days, $^{60}$Co, ssd = 75 cm, sep. 20 cm, equiv. sq. 16.2 cm.

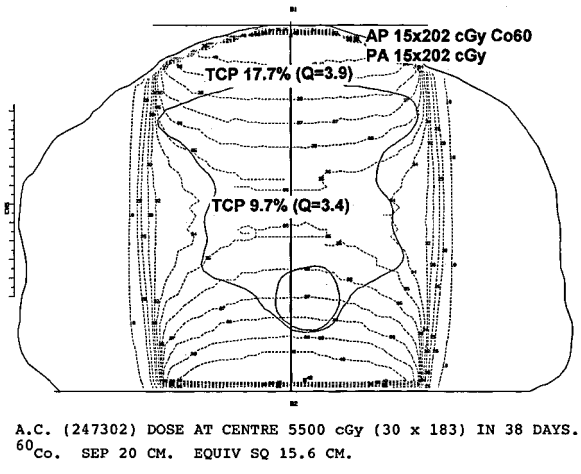


**Figure 10.13** Patient A.C. dose at center 5500 cGy, in 38 days, $^{60}$Co, ssd = 75 cm, sep. 20 cm, equiv. sq. 15.6 cm.

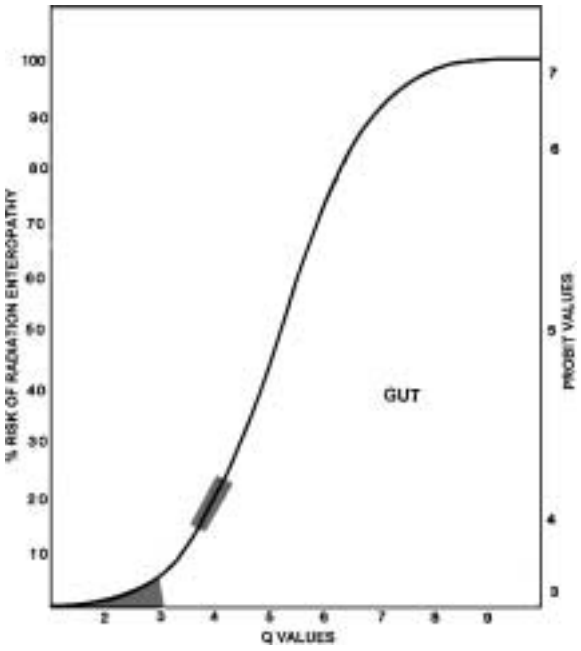


**Figure 10.14** The cases in figures 10.5–10.13 (rectangular box) and the estimated % risk of radiation enteritis using the CPK multi-target model for gut.

### 10.5.2 CPK Multi-Target Model Used to Demonstrate the Volume Effect in Gut

Figures 10.15–10.17 demonstrate the volume effect as applied to gut tolerance using the Cohen CPK multi-target model. The nominal standard dose (NSD) equivalent isoeffect model for radiation enteropathy proposed by Cohen and Creditor (1983) is

$$\text{total dose} = 1582 \cdot N^{0.29} \cdot T^{0.08} \quad (10.1)$$
$$\text{(5\% probability of risk)}$$

where $N$ is the number of fractions and $T$ is the overall treatment time in days. From equation (10.1), 26 fractions of 208 rad per fraction for a "standard 10 cm field" has a probability of complication of 5%.

As described in chapter 1, Cohen and Creditor proposed a field size exponent ($y = 0.22$ for gut) for the "field size" treated, by which means a correction for volume could be made. In order to demonstrate the volume effect in gut, the Cohen CELKIL multi-target equation has been used in the bioeffect planning system in which the parameter values defined by Cohen and Creditor have been used ($D_0 = 1.64$, extrapolation number = 20, $L$ (day$^{-1}$) = 0.1, $K/J = 2.4$, $G$ (cycles) = 17, $y = 0.22$, interval between fractions 1.4).

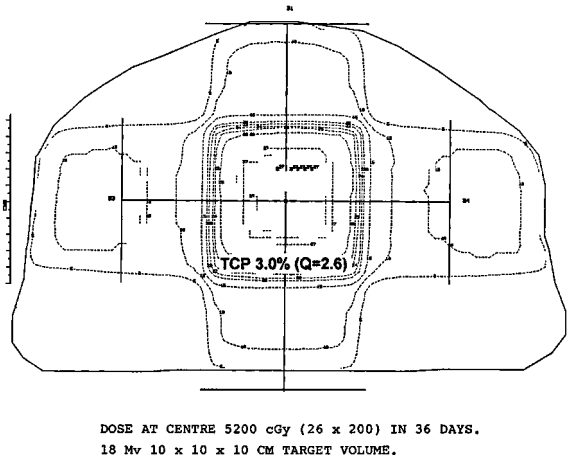


**Figure 10.15** Demonstration of the volume effect in gut with the dose at the isocenter 26 × 200 cGy in 36 days, 18 MV, 10 × 10 × 10 cm target volume. Complication probability 3%.

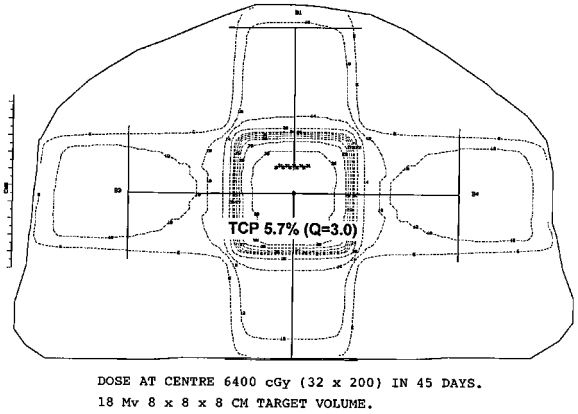


**Figure 10.16** As for figure 10.15 except the volume treated is 8 × 8 × 8 cm in 45 days. Complication probability 6%.

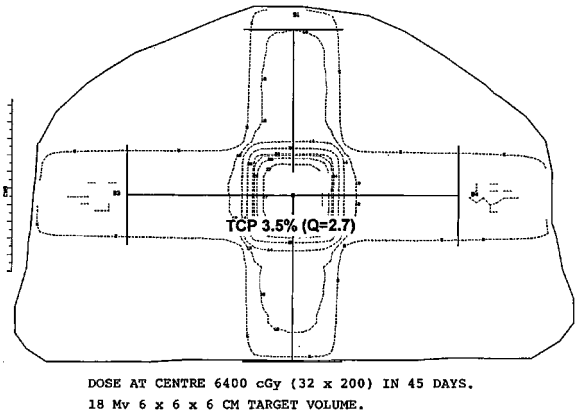


**Figure 10.17** As for figure 10.16 except that the target volume has been reduced to 6 × 6 × 6 cm. Complication probability 3.5%.

Figure 10.15 is a bioeffect plan for 26 fractions of 200 cGy given to the isocenter of a volume of gut equivalent to the standard reference volume of Cohen and Creditor ($10 \times 10 \times 10$ cm). This figure shows that the predicted complication probability was 3% ($Q = 2.6$) which is similar to the 5% complication probability proposed. In figure 10.16 the target volume has been reduced to $8 \times 8 \times 8$ cm and the number of fractions changed to derive a complication probability of approximately 6% ($Q = 3.0$). The number of fractions required to give this complication rate was found to be 32. A further reduction in the target volume to $6 \times 6 \times 6$ cm has been made in figure 10.17, and the complication probability was shown to fall to 3.5% ($Q = 2.7$). These estimates would appear consistent with clinical experience.

### 10.5.3 Disparities Between Dose and Effect in Parallel Opposed Fields Treating 1 or 2 Fields Daily Which are Not Apparent with Isodose Plans

Disparities between dose and biological effect may occur when all fields are not treated daily (Wigg and Wilson 1981). The practice of treating only one field daily in a parallel pair of fields was fairly common particularly when some early model linear accelerators were incapable of 180° rotation. As demonstrated below, standard isodose planning does not indicate any difference whether one or two fields are treated, but one field per day reduces workloads. As this practice was quite common even in the 1980s, bioeffect plans were generated in 1987 using a time dose fractionation (TDF) model for stroma described by Orton and Ellis (1973) and discussed in chapter 9, Tumor Control and Late Effect Predictive Models and Their Clinical Applications.

$$\mathrm{TDF} = N \cdot d_g^{1.538} \cdot x^{-0.169} \cdot 10^{-3} \tag{1.4}$$

where $N$ is the number of fractions given, $d_g$ is the dose per fraction, and $x$ is a function of the number of treatment days per week. This model permits the summation of partial treatments.

Figure 10.18 shows the twice daily treatment method using a 4 MV beam, ssd = 90 cm, the number of fractions $N = 28$, the dose per fraction exponent = 1.538, $x = 1.37$, the time exponent = –0.169, and a scaling factor = 1. Figure 10.19 shows the one field per day treatment technique in which $N = 14$ for both the anterior and posterior fields treated on alternate days. The bioeffect numbers shown in the two figures are TDF values normalized to 100% at the isocenter (the actual TDF values may be derived by multiplying these values by 1.089). The ratio of the predicted biological effect (in units of normalized TDF values) at the peak

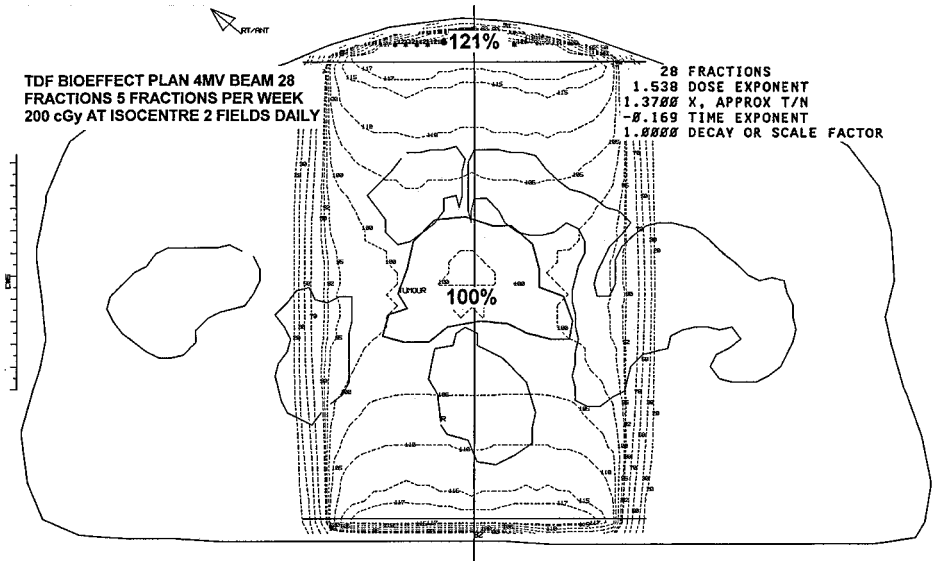


**Figures 10.18–10.20** Differences between bioeffect planning and isodose predictions when 1 or 2 fields per day are treated with a parallel pair of fields. The differences are shown as the ratios of the effect at the peak region to that at the isocenter. Parameter values of the bioeffect model used are also shown. Isodose planning underestimates the biological effect and does not differentiate between the techniques.

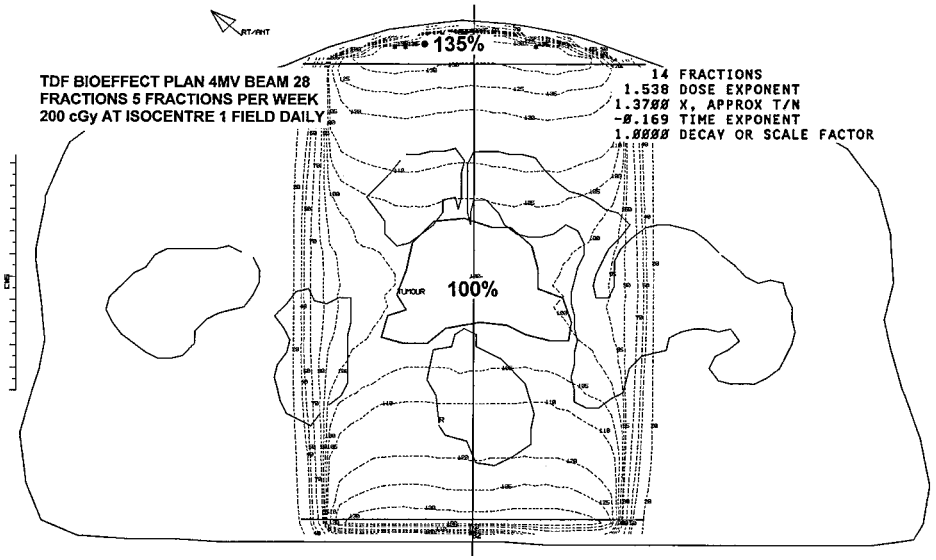


**Figure 10.19** See fig. 10.18.

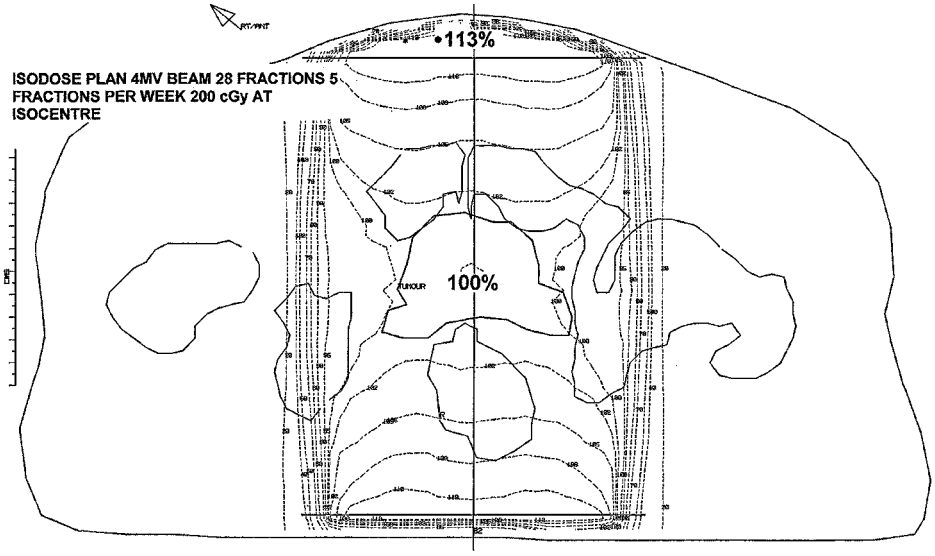


**Figure 10.20** See fig. 10.18.

region to that at the center when treating two fields per day was 1.21 compared with 1.35 for the technique treating one field per day.

Isodose planning, as shown in figure 10.20, does not differentiate between the two techniques. When treating one field per day the peak dose on one day required to deliver 200 cGy at mid separation was 351 cGy and the exit dose on the following day at this point was 100 cGy. Over two days the dose in the peak region averages 226 cGy per day (351 + 100)/2 compared with 200 cGy daily at the isocenter (ratio 1.13).

The biologically effective dose is fraction size dependent and the summation of two partial treatments, which, for the one field daily technique, includes alternately a comparatively large and small dose per fraction. This results in a higher biological effect than if the same total dose were given with both fields treated daily, in which case the same dose per fraction is given daily. In effect, with the one field daily technique, the alternate large fractions overcompensate for the small fractions. When treating two fields daily the daily dose in the peak region was $113/100 \times 200$ cGy = 226 cGy, as can be seen in figure 10.20. The biological effect of treating with daily fractions of 226 cGy shown in figure 10.18 is less than that treating with alternatively 351 and 100 cGy, as shown in figure 10.19. The ratio of biological effect at the peak region to the isocenter when treating both fields daily is 1.21 compared with 1.35 when treating one field daily. The magnitude of the disparities between effects predicted by isodose and bioeffect planning vary with, for example, beam quality. Table 10.1 summarizes

**Table 10.1** Ratio of dose or biological effect at the peak region to the center, in a parallel pair of fields. 18 and 4 MV at SAD = 100 cm. $^{60}$Co at SAD = 75 cm, 28 fractions 200 cGy per fraction at mid separation, five treatments per week

| | $^{60}$Co | 4 MV | 18 MV |
|---|---|---|---|
| Isodose | 1.24 | 1.13 | 1.04 |
| Bioeffect | | | |
| 2 fields daily | 1.39 | 1.21 | 1.07 |
| 1 field daily | 1.64 | 1.35 | 1.11 |

similar disparities between dose and effect for the same treatment using different beam qualities.

There are many variations of the technique of not treating all fields daily, such as treating only two fields in a four-field technique. The practice of not treating all fields daily carries with it the risk of increased biologically effective dose which is not identified with isodose planning, examples of which are described in section 10.5.1.

### 10.5.4 Tumor Control Probability Bioeffect Plans Using Mean Parameter Values

The relationship between the volume effect and tumor control probability (TCP) may be demonstrated by various methods using bioeffect planning. For example, as applied to gut, a variety of models may be used. While the linear-quadratic model is preferable, there is some uncertainty regarding an appropriate $\alpha/\beta$ value, so for the purpose of demonstration the modified variable exponent linear-quadratic factor (LQF) model expressing effects in terms of the number of fractions of 2.0 Gy per fraction, equation (1.14), is used. The tolerance dose to a reference volume of 10 $\times$ 10 $\times$ 10 cm is defined in this model as equivalent to 28 fractions of 2.0 Gy. From chapter 1, equation (1.14) defines the number of daily fractions $N_b$ of $d_s$ Gy per fraction that is biologically equivalent to $N$ fractions of $d_g$ Gy per fraction given to a partial volume defined by $L_t$.

$$N_b = N \cdot \left(1 + \frac{d_g}{r}\right) \cdot \left(\frac{L_t^3}{10^3}\right)^{\phi} \left[d_s^{-1} \cdot \left(1 + \frac{d_s}{r}\right)^{-1}\right] \qquad (1.14)$$

where

$N$ = the number of fractions given,

$d_g$ = the dose per fraction given,

$r = \alpha/\beta$ ratio of tissue specific for this model,

$d_s$ = the specified dose per fraction,

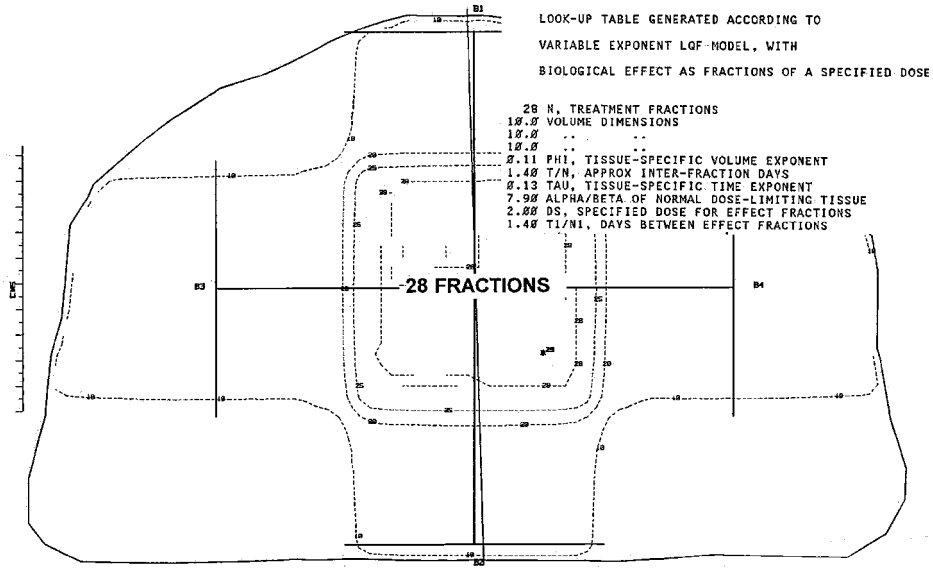


**Figure 10.21** A bioeffect plan using 28 fractions of 2.0 Gy to a $10 \times 10 \times 10$ cm volume which is defined as tolerance by the modified LQF model for gut.

$L_t$ = the side lengths of the target volume assuming it to be a cube,

$\phi$ = the tissue specific volume exponent.

Figure 10.21 shows the biological effect expressed in terms of the number of fractions ($N_b$) of $d_s$ = 2.0 Gy per fraction given to a reference volume of $10 \times 10 \times 10$ cm which is, as expected, equivalent to 28 fractions of 2.0 Gy per fraction. The parameter values used for the LQF model applied to gut are shown in table 1.1 and in figures 10.31 and 10.22. In figure 10.22 the volume was reduced to $8 \times 8 \times 8$ cm and 30 fractions of 2.0 Gy per fraction may be given to produce the same complication probability as 28 fractions of 2.0 Gy to a reference volume of 10 $cm^3$. Therefore, two extra fractions may be given to the smaller volume. Provided the same number of tumor clonogens are confined within the $8 \times 8 \times 8$ cm cube target volume the TCP will be increased by treating the reduced volume to tolerance. The potential increase in TCP for an individual case may be demonstrated by using equation (6.25).

$$\mathrm{TCP} = \exp[-\exp(-N \cdot \{\alpha \cdot d_h \cdot (1 + h_m) + \beta \cdot [d_h \cdot (1 + h_m)]^2\})M \cdot 2^{T/Tp}] \quad (6.25)$$

where

$N$ = the number of fractions,

$\alpha$ and $\beta$ = the tumor radiosensitivity factors,

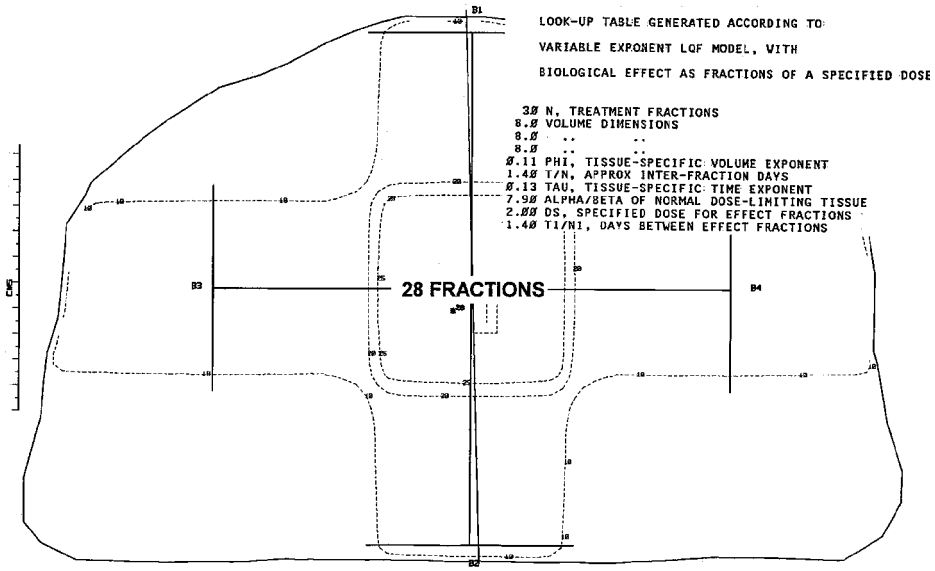


**Figure 10.22** A bioeffect plan showing that 30 fractions of 2.0 Gy to an $8 \times 8 \times 8$ cm volume of gut is isoeffective with 28 fractions of 2.0 Gy to a $10 \times 10 \times 10$ cm target volume.

$h_m$ = the incomplete repair factor (for hyperfractionated treatments),

$d_h$ = the dose per fraction given,

$M$ = the tumor clonogen number,

$T$ = the overall treatment time,

$T_p$ = the average doubling time of tumor clonogen in days.

Figure 10.23 is a bioeffect plan using equation (6.25), the parameter values are shown in figures 10.23 and 10.24. Figure 10.33 shows that a TCP of 2% is achieved treating $10^{13}$ clonogens using a $10 \times 10 \times 10$ cm target volume. The $\alpha/\beta$ value of the tumor used was 0.402/0.049 Gy and a tolerance dose of 28 fractions of 2.02 Gy per fraction was used. In order to bring the TCP slightly above 0, 2.02 Gy per fraction was used rather than 2.0, as using 2.0 Gy was just too low for the planning computer to print a satisfactory plan. In the example shown $T$, $T_p$, and $h_m$ were all assumed to be 0, although the option exists for hyperfractionation and repopulation factors to be used. The $\alpha/\beta$ value used for the tumor was the average value for human colonic carcinoma (Fertil and Malaise 1981). Figure 10.24 shows that the TCP is increased to 50% if an extra two fractions are given, consistent with the increase in dose that can be given with a volume reduction to an 8-cm cube.

Equation (6.25) may be used to demonstrate the effects of tumor repopulation and also accelerated or hyperfractionated treatment. For example, figures 10.25–10.28 are a series of bioeffect plans in which stromal

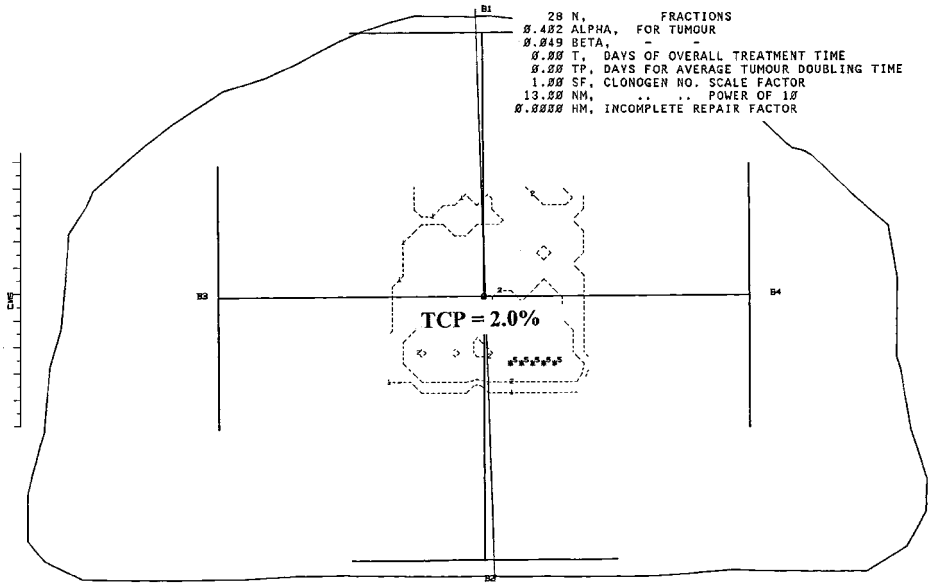


**Figure 10.23** A bioeffect plan showing tumor control probability. The dose is determined by the volume of gut irradiated. ($10 \times 10 \times 10$ cm, $28 \times 2.02$ Gy to $10^{13}$ clonogens, $\alpha/\beta = 0.402/0.049$ Gy).

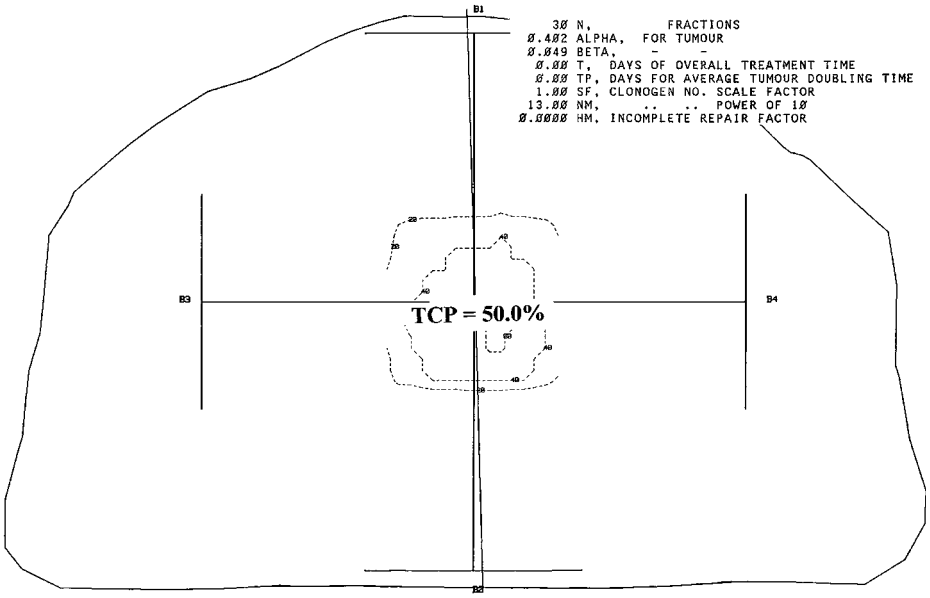


**Figure 10.24** A bioeffect plan showing tumor control probability. Dose determined by volume of gut irradiated. ($8 \times 8 \times 8$ cm, $30 \times 2.0$ Gy to $10^{13}$ clonogens, $\alpha/\beta = 0.402/0.049$ Gy).

($\alpha/\beta = 3.0$ Gy) tolerance doses to an assumed $10 \times 10 \times 10$ cm volume were given. Doses biologically equivalent to 30 fractions of 2.0 Gy have been used. These equivalent doses were determined with the EFFECT model, alternatively the "look-up" graph in figure 1.3 could be used. The doses

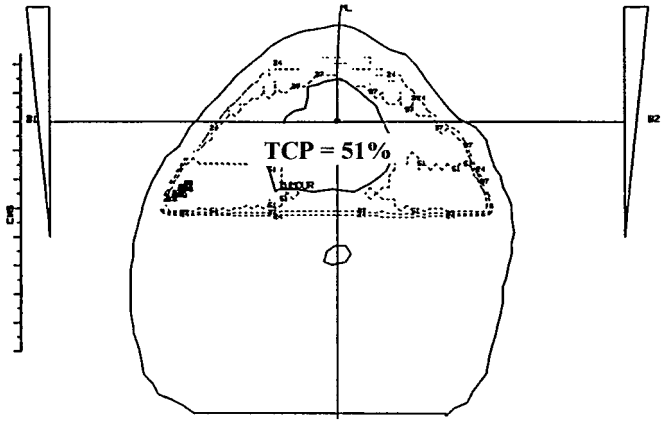


**Figure 10.25** A TCP bioeffect plan using equation (6.25). Thirty-five fractions of 1.8 Gy were given resulting in a TCP within the target volume of 51%.

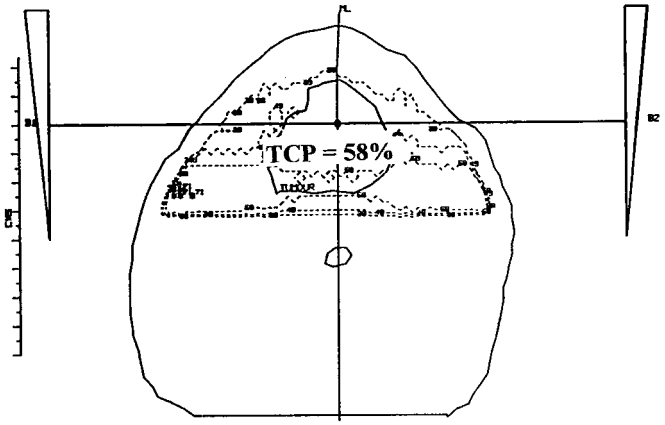


**Figure 10.26** A TCP bioeffect plan in which a biologically equivalent dose to stroma has been given using 25 daily fractions of 2.3 Gy per fraction. This results in a small rise in TCP to 58%.

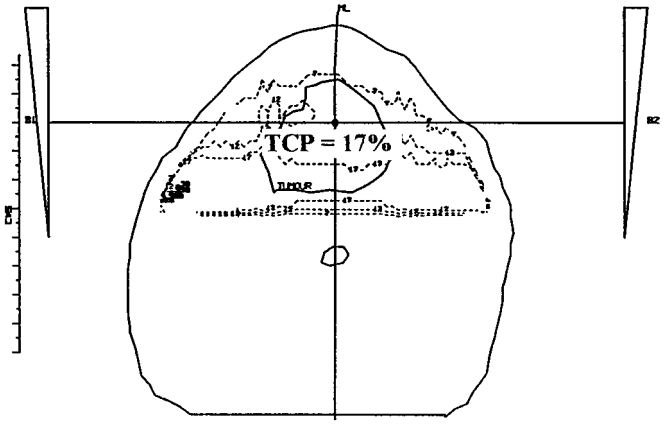


**Figure 10.27** A TCP bioeffect plan in which the biologically equivalent dose to stroma given was 15 daily fractions of 3.2 Gy per fraction. The TCP has fallen to 17%.

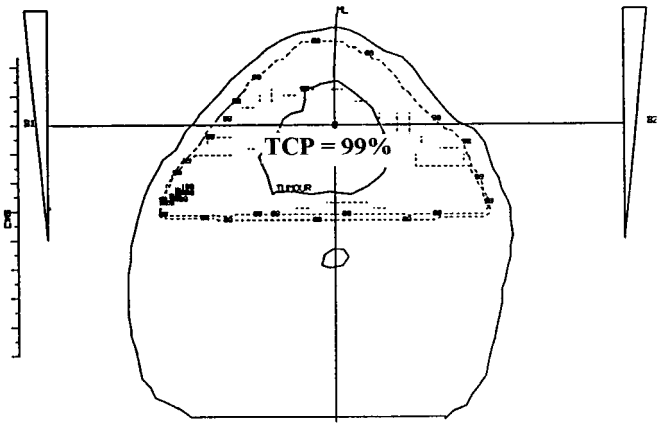


**Figure 10.28** A TCP bioeffect plan in which 70 fractions treated twice daily using 1.05 Gy per fraction has been used. There is a substantial increase in TCP to 99%.

used were 35 daily fractions of 1.8 Gy, 25 daily fractions of 2.3 Gy, and 15 daily fractions of 3.2 Gy. The clonogen number was assumed to be $10^{10}$, the tumor $\alpha/\beta$ value was assumed to be 0.38/0.042 Gy, and the average doubling time of the tumor cells assumed to be 6 days. Figure 10.25 shows that using 35 fractions in 49 days a TCP of 51% is achieved; an increase in TCP to 58% is shown in figure 10.36 by reducing the overall treatment time to 25 fractions in 35 days, but 15 fractions in 21 days results in a fall in TCP to 17%, as seen in figure 10.37. Twice daily treatments with 70 fractions of 1.05 Gy with an $h_m$ of 0.063 result in a substantial increase in TCP to 99%, as shown in figure 10.38.

Figures 10.25–10.28 show an initial progressive rise in TCP as the average treatment time of daily fractions is decreased, but a fall in TCP if the overall treatment time is reduced excessively, for example, to 21 days in this example. It should be noted that in the examples shown in figures 10.21–10.38 the effects of inhomogeneities of tumor parameter values have not been included, but as the target volume was small the dose was relatively homogenous and the effect of introducing variability of parameter values is likely to be relatively small. These results and the benefit of twice daily treatments are discussed in chapter 6, The Effects of Time and Repopulation During the Treatment Period on Tissue Responses, Tumor Control Probability, and Optimum Fractionation.

The OPTIMUM model may be used to predict the likely TCP when the variables are the same as in figures 10.25–10.28. It may also be used to derive the optimum fractionation for each schedule of treatment. The optimum fractionation is 27 × 2.2 Gy for the daily treatments and 60 × 1.18 Gy for the hyperfractionated treatments.

The above examples demonstrate the potential use of bioeffect planning in which the end result is quantified in terms of TCP, but without including the effects of inhomogeneities of parameter values on TCPs. The effects of inclusion of these inhomogeneities on TCP predictions are shown in sections 10.5.5, 10.5.6, and 10.5.8.

### 10.5.5 Isodose and Bioeffect Planning for Whole Brain Irradiation

Although skull shapes are quite variable, the typical adult skull is approximately hemispherical. When the whole brain is treated with a parallel pair of fields, the separation values decrease from the center superiorly and antero-posteriorly. Consequently, the isodose and dose per fraction distribution may be quite variable. As was shown in table 8.7, human brain has a relatively high fractionation sensitivity ($\alpha/\beta = 2.0$ Gy), so variations in fraction size will significantly affect the biologically effective dose when using a parallel pair of fields.

Figure 10.29 is an isodose plan in which a 6 MV beam is used, ssd = 100 cm, with the dose normalized to 100% at the isocenter and figure 10.30 is a dose display in the same plane. In both examples the dose increases up to 6% in the high dose region. Figure 10.31 is a dose display 4.0 cm superior to figure 10.30 and shows that the dose per fraction increases up to 227 cGy, which is 13.5% higher than at the isocenter in figure 10.30.

Figure 10.32 is a bioeffect plan using a modified linear-quadratic based fractionation dosage factor (FDF) model, equation (1.19). Twenty-five fractions of 2.0 Gy were prescribed at the isocenter, $\alpha/\beta = 2.0$ Gy, from table 8.8, $\phi = 0.9$, and the treatment volume and reference volume were

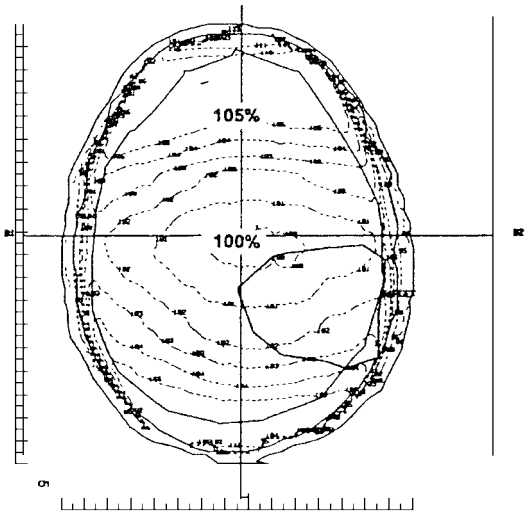


**Figure 10.29** An isodose plan with the dose normalized to 100% at the isocenter. 6 MV beam used.

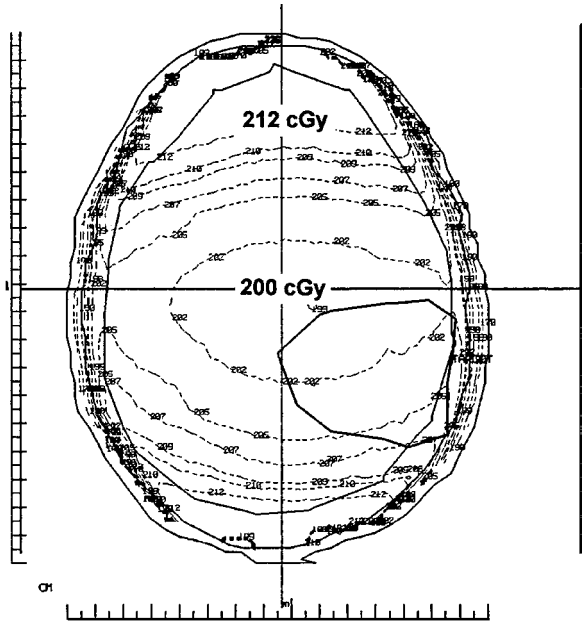


**Figure 10.30** A dose per fraction plan for the same slice as figure 10.29. The dose per fraction is in cGy.

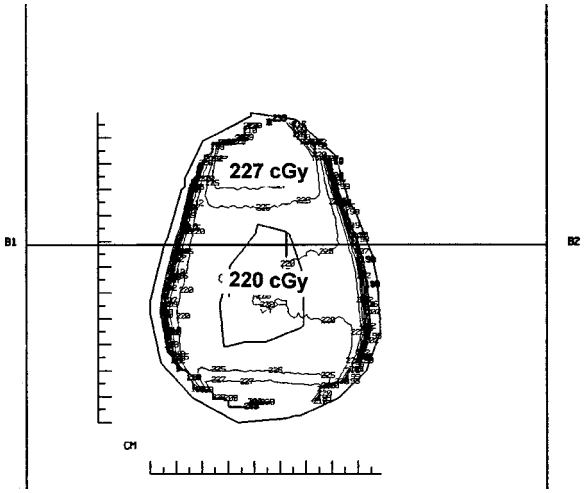


**Figure 10.31** A dose per fraction plan in a plane 4.0 cm superior to figure 10.30.

each assumed to be $10 \times 10 \times 10$ cm. As the specified dose per fraction $d_s$ = 2.0 Gy, the biologically effective dose is expressed in terms of a number of fractions of 2.0 Gy. Figure 10.32 shows a biologically effective dose of 25 fractions at the isocenter which increases to 28 fractions anteriorly representing an increase of 12%. Figure 10.33 is a bioeffect display 4.0 cm superior to figure 10.32 and shows an increase up to 32 fractions which is 28% higher than at the isocenter in figure 10.32. In this example

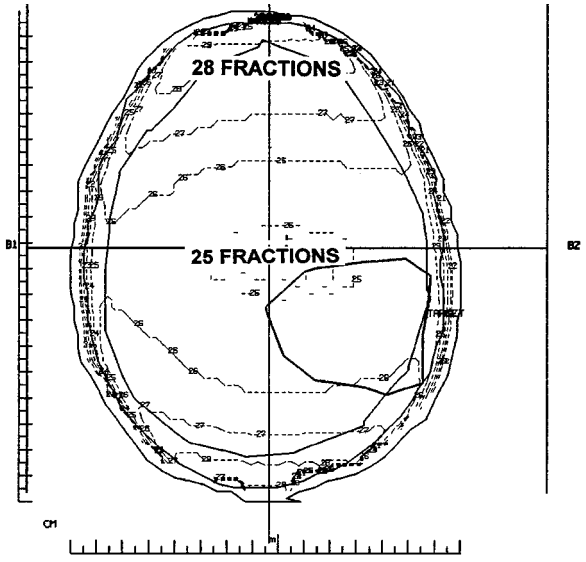


**Figure 10.32** A bioeffect plan of figure 10.30 with the biologically effective dose defined as the number of fractions of 200 cGy. Twenty-five fractions of 200 cGy were prescribed as the isocenter.

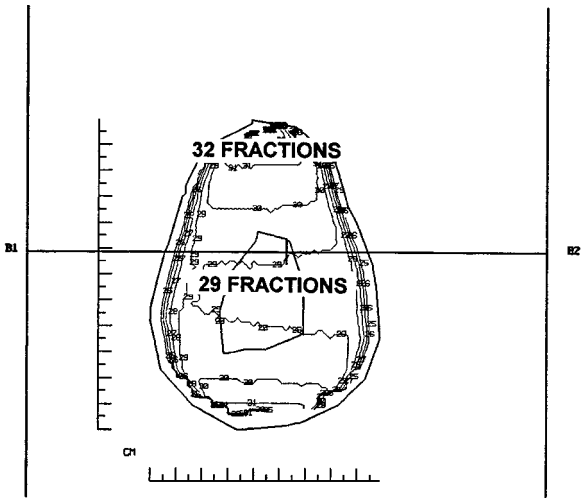


**Figure 10.33** A bioeffect plan at 4.0 cm superior to figure 10.32.

bioeffect planning shows a substantially greater variation in effect on brain tissue than would be appreciated from isodose planning. This effect can be almost eliminated by compensating filters, as shown in figure 10.34, which shows that even in the vertex region the effective dose is between 24 and 25 fractions of 2.0 Gy. Although not shown in these figures, when compensating filters are used, the variation in biologically effective dose throughout the whole brain may be reduced to between 24 and 25 fractions of 2.0 Gy.

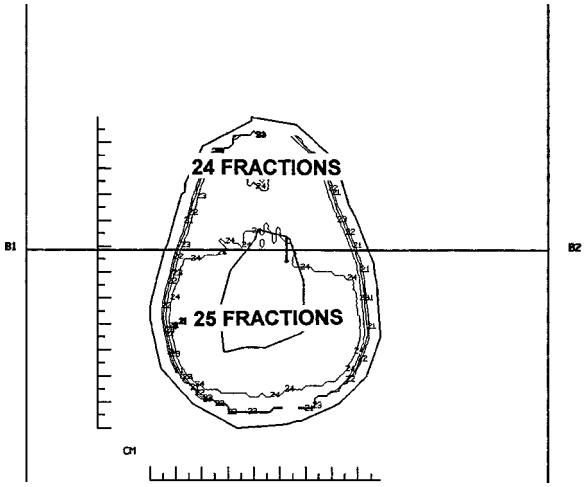


**Figure 10.34** A bioeffect plan of figure 10.33 but a compensator has been used for the whole brain.

The effect of variation in dose per fraction on TCP may be examined using equation (9.9) in the EFFECT model described in chapter 9. This model includes a flattening effect of parameter inhomogeneities on TCP predictions. If parameter inhomogeneities are excluded from these calculations, the predicted variability of TCP within the brain would be higher. In the following examples it was assumed that a typical carcinoma, as described in figure 9.11, lies within the brain and the TCP is calculated assuming uniform clonogen cell density. The values used were $\alpha_m = 0.35$, $\alpha_\sigma = 0.088$ Gy$^{-1}$, $\beta_m = 0.042$, $\beta_\sigma = 0.029$ Gy$^{-2}$, $T_{pm} = 4.7$, $T_{p\sigma} = 3.2$, $T_0 = 46.2$, $T_s = 0$, $T_k = 7$ days, $d_{g\sigma} = 0.05$ Gy, $h_{mt} = 0$. Clonogen cell numbers $M_m$ were $10^7 \times 3.5^3$ and were sufficient to give a TCP within the stochastic region in the TCP curve.

Figure 10.35 shows that the TCP varies from 48% to 54%. In the plane near the vertex the TCP varies between 57% and 66%, as shown in figure 10.36. This big variation of TCP within the brain is reduced when compensating filters are used, in which case the TCP throughout the whole brain lies between 46% and 49%, as shown in figure 10.37.

Table 10.2 is a summary of these findings. In each comparison isodose planning underestimates the biological effect in normal brain tissue with the isodose percent difference being approximately half the bioeffect prediction. These differences were practically eliminated with compensating filters. The predicted TCP varied between 47% and 66% without compensators, reducing to 46–49% when compensators were used.

Uncompensated parallel pairs of fields to whole brain are widely used. In these examples bioeffect planning clearly shows the underestimation of the effects of this technique if compensators are not used. If chemotherapy

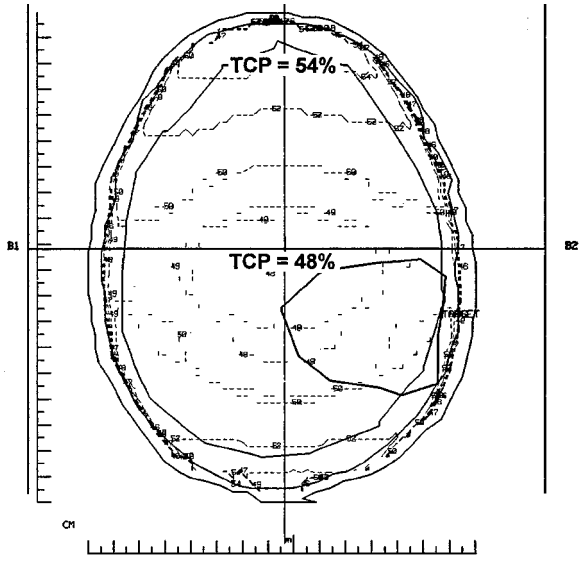


**Figure 10.35** A tumor control probability plan showing a variation of TCP from 48–54% in this plane.

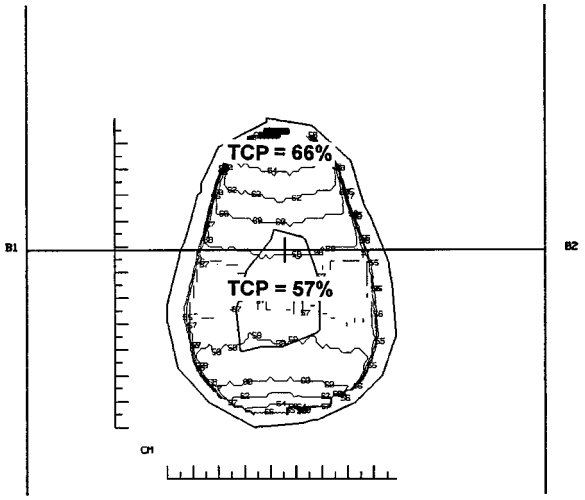


**Figure 10.36** A tumor control probability plan in a plane 4.0 cm superior to figure 10.35. The tumor control probability varies from 57% to 66%.

is used in addition to radiotherapy, the biologically effective dose would be further increased by an unquantifiable amount in the absence of reliable dose-modifying effect values. Late brain effects following whole brain irradiation, especially when combined with chemotherapy, have been a matter of concern for many years. It is suggested that the high biologically effective doses in the regions of reduced separation are undesirable and that compensating filters would reduce this hazard.

**Table 10.2** Differences in predicted effective dose in normal brain when isodose or bioeffect plans are used. Also shown are predicted tumor control probabilities. No tissue compensators used

| | Dose plan | Bioeffect plan |
|---|---|---|
| High dose region vs. isocenter. Central slice | +6% | +12% |
| High dose region vs. isocenter. Slice near vertex | +3.2% | +10.3% |
| High dose region in vertex vs. dose at isocenter | +13.5% | +28% |

Variation in tumor control probability throughout whole brain 47–66% without compensator, 46–49% with compensator

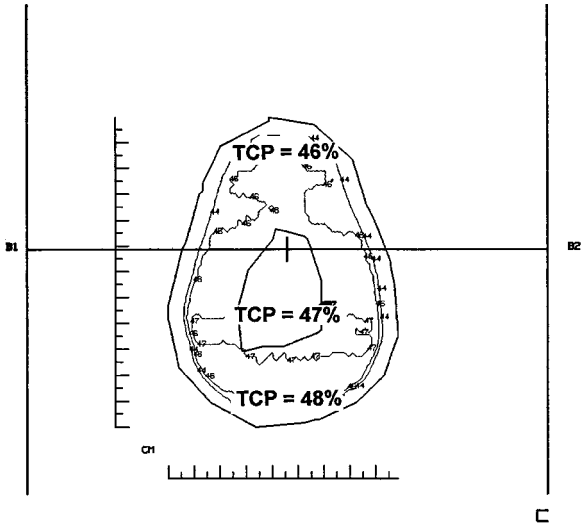


**Figure 10.37** A tumor control probability plan in the same plane as figure 10.36. Tissue compensators have been used and the tumor control probability throughout the whole brain now varies much less and is between 46% and 49%.

### 10.5.6 Disparities Between Isodose and Bioeffect Predictions when Treating the Vertebral Column with Posterior Fields

A single posterior field is frequently used when treating the vertebral column; for example, for palliation of vertebral metastases. It is not always fully appreciated how much the biologically effective dose falls with depth with this simple technique. For example, figures 10.38–10.40 and 10.42–10.44 show both the isodose and bioeffect predictions for 6- and 18 MV and $^{60}$Co beams, in which a dose of 23 fractions of 2.0 Gy was prescribed to the lower end of the spinal cord at a depth of 5 cm ($D$ = 5.0 cm). The model used to express the biologically effective dose as the

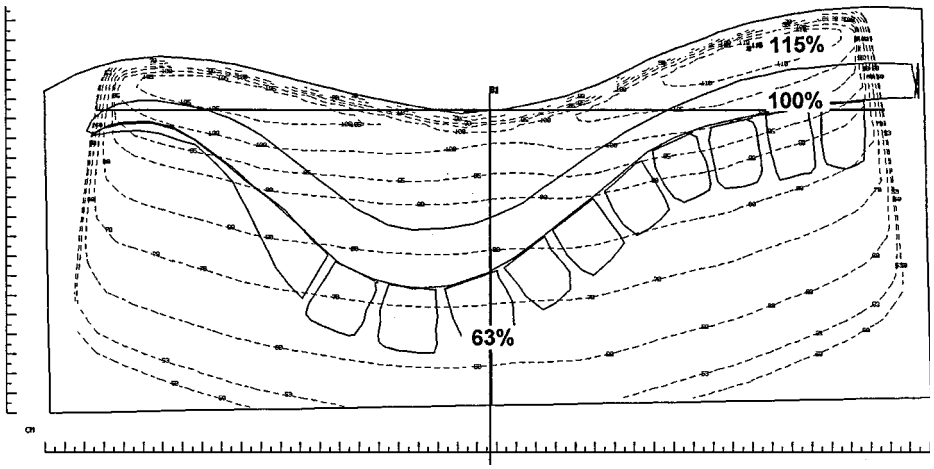


**Figure 10.38** An isodose plan, 6 MV beam, 40 × 8.0 cm, ssd = 100 cm, 100% at $D = 5.0$ cm.

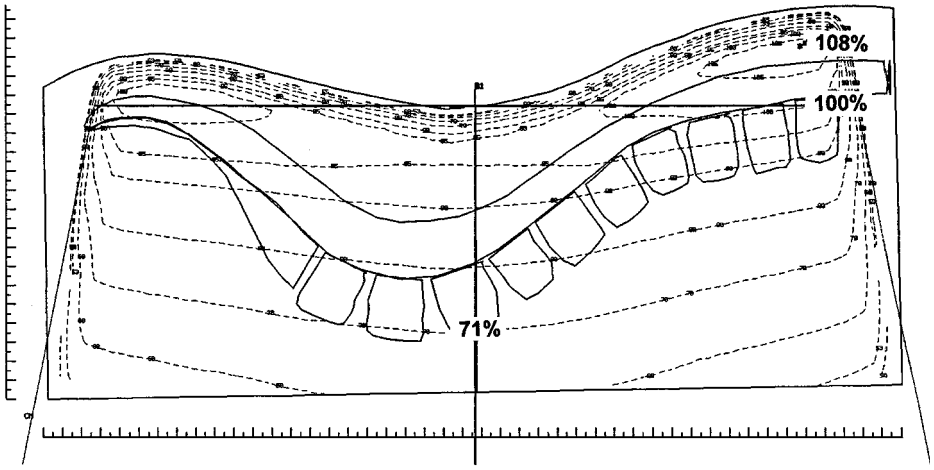


**Figure 10.39** An isodose plan, 18 MV beam, 40 × 8.0 cm, ssd = 100 cm, 100% at $D = 5.0$ cm.

number of fractions of $d_s$ Gy is described in chapter 1, equation (1.19) and figure 1.3.

$$N \cdot d_g \cdot (r + d_g) \cdot \left(\frac{L_t^3}{L_r^3}\right)^{\phi} \cdot (r + d_s)^{-1} \cdot d_s^{-1} \qquad (1.19)$$

In the examples shown the number of fractions prescribed $N = 23$, the $\alpha/\beta$ value of the tissue considered $r = 3.0$ Gy, the volumes were assumed to be the same as the reference volume $10 \times 10 \times 10$ cm, the tissue-specific volume exponent $\phi = 0.80$ for stroma, and the specified dose per fraction $d_s$ was 2.0 Gy.

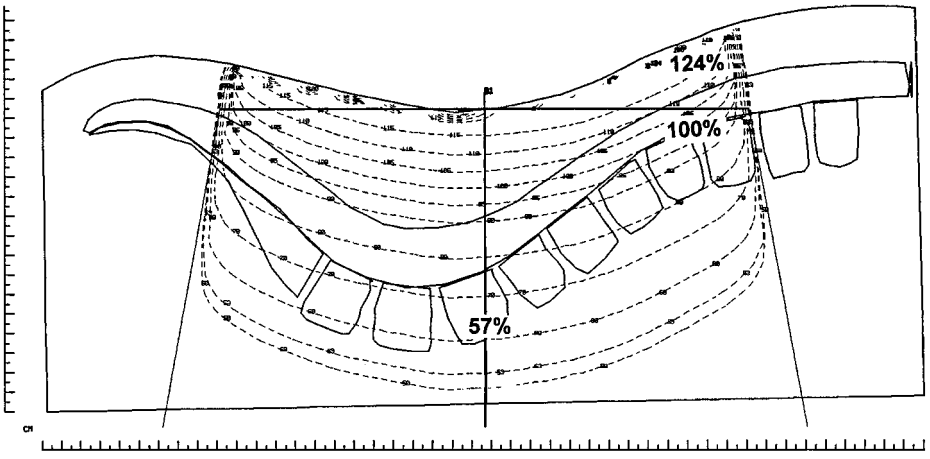


**Figure 10.40** An isodose plan, $^{60}$Co beam, 27 × 8.0 cm (max. field length available), ssd 75 cm, 100% at $D$ = 5.0 cm.

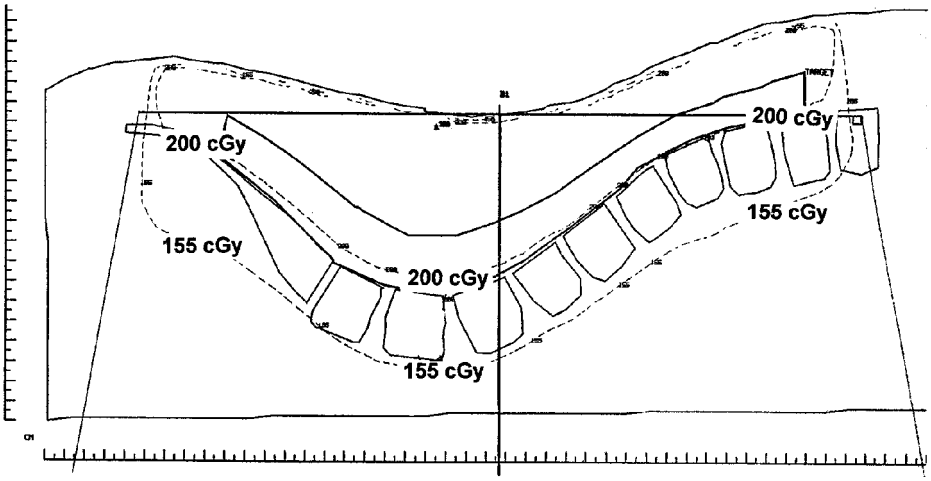


**Figure 10.41** A compensated "rad display," 4 MV beam, 40 × 8.0 cm, ssd = 100 cm, 200 cGy at $D$ = 5.0 cm.

Figure 10.38 shows that when the dose is normalized at $D$ = 5.0 cm, the percent dose at the anterior border of the third lumbar vertebra (L3) is 63%, but the biologically effective dose at the anterior border of L3 is the equivalent of 12 × 2.0 Gy compared with 23 × 2.0 Gy at D = 5.0, as shown in figure 10.42. The biologically effective dose is less than that predicted by the isodose plan being 52% of the prescribed dose, as is shown in table 10.3. The fall in dose and biological effect comparing the peak dose region and the vertebral body region is larger, and again the bioeffect plan shows that isodose planning underestimates this effect. Table 10.3 summarizes figures 10.38–10.40 and 10.42–10.44 for $^{60}$Co, 6 MV, and 18 MV beams.

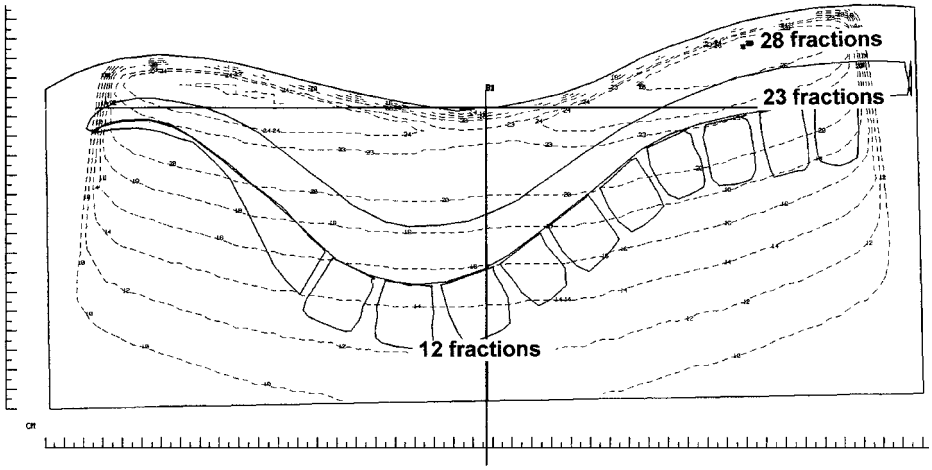


**Figure 10.42** A bioeffect plan expressed as a number of fractions of 200 cGy, 6 MV beam, ssd = 100 cm, 23 × 200 cGy at $D = 5.0$ cm.

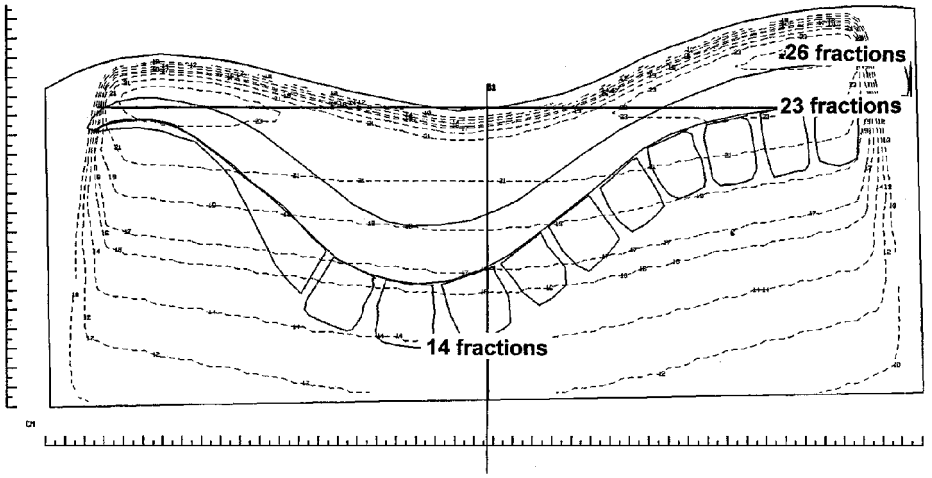


**Figure 10.43** A bioeffect plan expressed as a number of fractions of 200 cGy, 18 MV beam, ssd = 100 cm, 23 × 2.0 Gy at $D = 5.0$ cm.

For each beam quality a large drop in dose and effect in the vertebral body occurs, especially with $^{60}$Co beams where the effective dose in the vertebral body is <50% of the prescribed dose (11 fractions vs. 23 fractions of 2.0 Gy in figure 10.44). For the 18 MV beam the effective dose in the vertebral body is increased to 14 × 2.0 Gy as in figure 10.43. Bioeffect plans show that this reduction is larger than the isodose plans would suggest. Even for palliative treatments of vertebral metastases, care must be taken that an adequate biologically effective dose is delivered, especially when using low energy and $^{60}$Co beams.

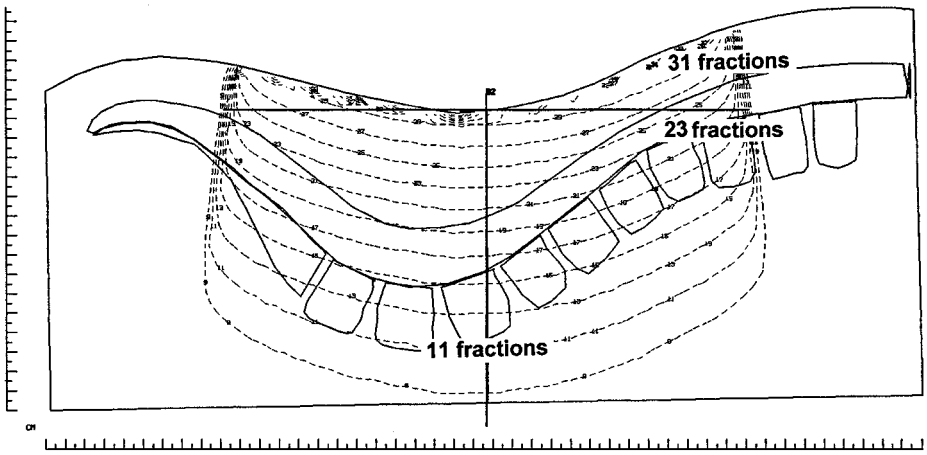


**Figure 10.44** A bioeffect plan expressed as a number of fractions of 200 cGy, $^{60}$Co beam, ssd = 75 cm, 23 × 200 cGy at $D$ = 5.0 cm.

**Table 10.3** Comparison of the biologically effective dose and isodose distributions when treating the vertebral column with a single posterior field of 23 fractions of 2.0 Gy at D = 5.0 cm

| Comparison between effect at D = 5.0 cm and anterior border of vertebral body L3 | | | Comparison between effect at the peak dose region and anterior border of vertebral body L3 | | |
|---|---|---|---|---|---|
| | Dose % | Bioeffect (Number of fractions of 2.0 Gy) | | Dose % | Bioeffect (Number of fractions of 2.0 Gy) |
| $^{60}$Co Beam | | | | | |
| Ant. body (a) | 57 | 11 | Ant. body (a) | 57 | 11 |
| D = 5.0 cm (b) | 100 | 23 | Peak dose (c) | 124 | 31 |
| Ratio (a/b) | 57 | 48% | Ratio (a/b) | 46 | 36% |
| 6 MV Beam | | | | | |
| Ant. body (a) | 63 | 12 | Ant. body (a) | 63 | 12 |
| D = 5.0 cm (b) | 100 | 23 | Peak dose (c) | 115 | 28 |
| Ratio (a/b) | 63 | 52% | Ratio (a/b) | 55 | 43% |
| 18 MV Beam | | | | | |
| Ant. body (a) | 71 | 14 | Ant. body (a) | 71 | 14 |
| D = 5.0 cm (b) | 100 | 23 | Peak dose (c) | 108 | 26 |
| Ratio (a/b) | 71 | 61% | Ratio (a/b) | 66 | 54% |

Figure 10.41 is a dose display in which a tissue compensator has been used to deliver 200 cGy to the spinal cord and cauda equina. In this example a 4 MV beam, ssd = 100 cm, has been used. If the biologically effective dose in the spinal cord is of interest, an $\alpha/\beta$ value of $r$ = 2.0 Gy could be used in equation (1.19). Clinically there are circumstances when it is important to determine the dose to the spinal cord; for example, when

treating the spinal axis in a medulloblastoma case. Under these conditions a compensator is desirable to deliver a uniform biologically effective dose to the spinal cord.

One of the consequences of the reduction in dose, and importantly the larger reduction biological effect at depth when using a single posterior beam, is the additional effect on TCP. Equation (9.9) from the EFFECT model has been used to estimate the TCP, as shown in figure 10.45. This model predicts a more conservative variation of TCP with variation in dose than equation (9.42), which does not include the flattening of TCP curves by inhomogeneities of parameter values. The parameter values used in figures 10.45 and 10.46 are the same as those used in figure 10.55

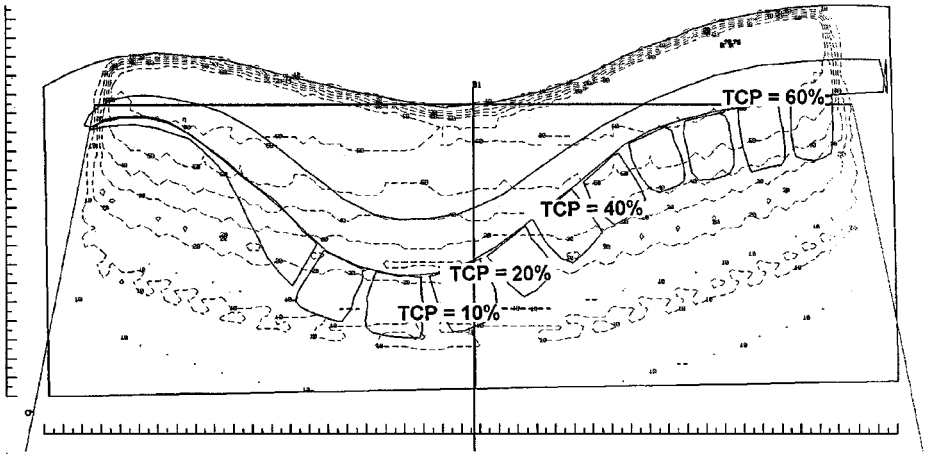


**Figure 10.45** The reduction in tumor control probability in the vertebral column with depth when 27 fractions of 2.0 Gy are delivered to $D = 5.0$ cm using a 6 MV beam.

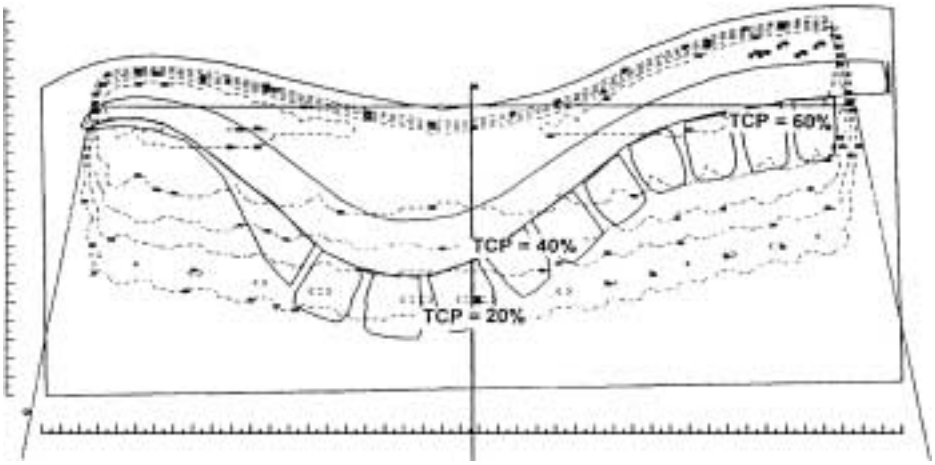


**Figure 10.46** Same as figure 10.45 except that an 18 MV beam has been used. There is less reduction in tumor control probability at depth but still a substantial drop occurs.

for TCP predictions, and the clonogen numbers have been adjusted to give a 60% TCP at the prescribed point at $D$ = 5.0 cm depth. Although the absolute number of clonogens is unknown, this method does permit comparison of the variations of TCP as the dose per fraction varies with depth.

Figure 10.45 shows that when using a 6 MV beam giving 27 fractions of 2.0 Gy at $D$ = 5.0 cm, the TCP in the vertebral column varies between 60% and 10%. Figure 10.46 shows the effect of delivering the same dose using an 18 MV beam. The reduction in TCP at depth is less but still very substantial.

### *Triple Trouble*

Examination of figures 10.38, 10.42, and 10.45 show a 3-stage progressing decline in predicted effects at the anterior body of L3 compared with the effects at $D$ = 5.0 cm at $D$9 vertebral body. When a 6 MV beam is considered, isodose planning predicts that the effect at L3 is 63% of that at $D$ = 5.0 cm. When a bioeffect plan describing the biological effect in normal tissues, as the equivalent of a number of 2.0 Gy fractions is used, the predicted effect drops to 52% at L3 compared with the effect at $D$ = 5.0 cm. When the predicted effect on tumor is considered in terms of TCP, the predicted effect drops further to 17%. As shown in table 10.4, these differences are less with an 18 MV beam, but are still substantial.

In terms of likely outcome of treatment this 3-stage reduction in effect may be considered to be potential "Triple Trouble," which is not apparent without bioeffect planning. The extent of this effect will vary for each case and depend on the treatment technique, normal tissue and tumor parameter values, and the models used.

From the above discussion large variation in dose and even larger variation in biologically effective and TCP occurs when a single posterior field is used to treat long lengths of the vertebral column. Bioeffect planning describes these effects better than isodose planning and also demonstrates the need for compensating filters when uniform effects are required.

**Table 10.4** Demonstration of a 3-stage (triple trouble) divergence of predicted effect between isodose planning, bioeffect planning predicting late effects in normal tissue defined in terms of an equivalent number of fractions of 2.0 Gy and tumor effects described in terms of tumor control probabilities. The results describe the ratio of effect at the anterior body of L3/effect at D = 5.0 cm at D9

| Beam Quality | Ratio of predicted effect using isodose plan (%) | Ratio of predicted late effects in normal tissues (%) | Ratio of predicted effect on tumor (TCP) (%) |
|---|---|---|---|
| 6 MV beam | 63 | 52 | 17 |
| 18 MV beam | 71 | 61 | 33 |

### 10.5.7 Limitations of Isodose Planning for Treating the Chest Wall and Axilla for Breast Carcinoma

#### *Axilla*

A common method of prescribing treatment to the axilla and supraclavicular fossa has been described by Perez et al. (1992), an example of which is shown below.

The treated volume in this region includes the apex of the lung, but delineation of this is frequently omitted due to difficulties associated with obtaining CT scans in the treatment position. A typical prescription is to deliver 50.0 Gy at 2.0 Gy per fraction at a depth of 3.0 cm using an anterior field combined with a reduced posterior field to supplement the dose to the midplane to deliver a total dose of 50.0 Gy at this point. This technique results in an additional exit dose anteriorly from the posterior field which increases the fraction size anteriorly to >2.0 Gy per fraction, especially if the posterior field includes lung tissues.

Figure 10.47 is an isodose display showing the dose per fraction contours expressed in cGy, when 25 fractions of 2.0 Gy was prescribed as above using a 4 MV beam, ssd = 100 cm, separation 17.0 cm, and corrected for lung tissue. The dose per fraction at mid separation was 200 cGy, at the peak region it was 250 cGy, and in the region of the brachial plexus it was approximately 242 cGy.

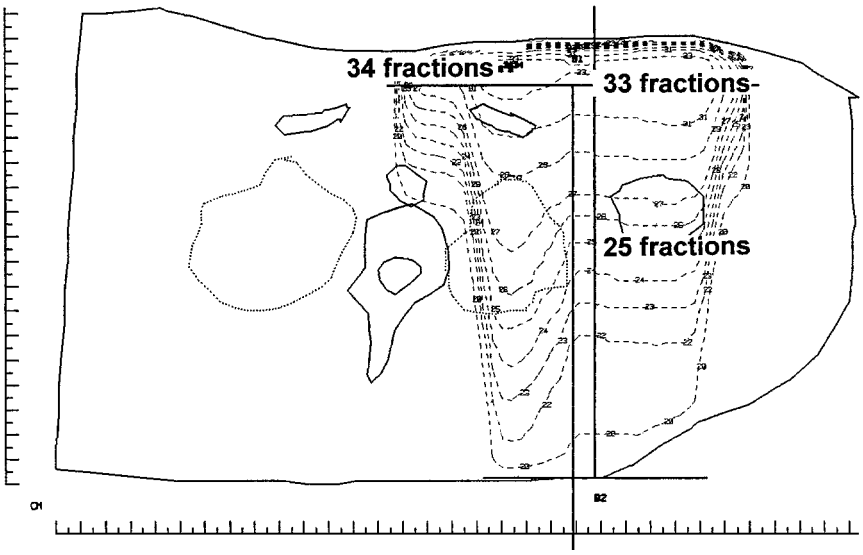


**Figure 10.47** A dose display plan with dose per fraction in cGy using a 4 MV beam, 50.0 Gy at 2.0 Gy per fraction prescribed at 3.0 cm depth anteriorly and boosted posteriorly to 50.0 Gy at mid separation. See text for details.

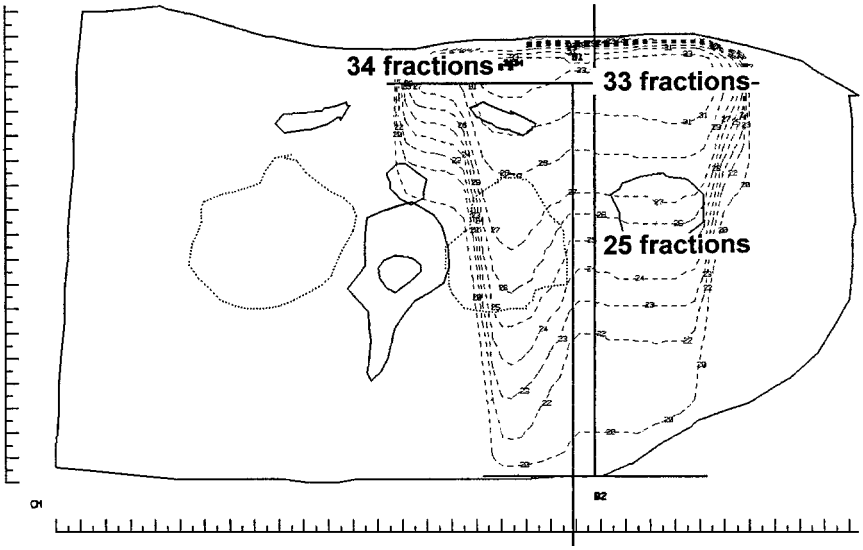


**Figure 10.48** A bioeffect plan for the same treatment shown in figure 10.47. The biologically effective dose is described as the equivalent number of fractions of 2.0 Gy per fraction.

Figure 10.48 is a bioeffect plan using equation (1.19) (number of fractions = 25, $\alpha/\beta = 3.0$ Gy, volume treated was assumed to be the same as the reference volume, $10 \times 10 \times 10$ cm, $\phi = 0.08$, and $d_s = 2.0$ Gy). The units of biological effect are the equivalent number of 2.0 Gy fractions. Figure 10.48 shows that anteriorly the hot spot received the equivalent of 34 fractions and a substantial volume in the region of the brachial plexus received the equivalent of 33 fractions of 2.0 Gy. The effect of lung corrections is quite small anteriorly and is equivalent to one fraction of 2.0 Gy because most of the dose is delivered by the anterior field. Further posteriorly the effect of lung tissue is more apparent.

Higher doses, for example up to 60.0 Gy at 2.0 Gy per fraction, are recommended if residual disease is present in the axilla. If 27 fractions are prescribed, the biologically effective dose in the brachial plexus region increases to the equivalent of 35 fractions of 2.0 Gy.

Table 10.5 shows the biological effect assessed by isodose and bioeffect planning for several beam qualities uncorrected for lung density. Twenty-five fractions of 2.0 Gy were prescribed as above, ssd = 100 cm for linear accelerated beams, and 75 cm for $^{60}$Co beams, separation 14 cm. Clearly, the high biologically effective dose anteriorly decreases as the energy increases, a factor of increasing importance as the separation increases. Again isodose planning underestimates the effect compared with bioeffect planning.

**Table 10.5** The effect of beam quality on the biological effect when treating the axilla and supraclavicular fossa. No lung corrections have been made

| | Comparison of effect at the peak region with the effect at mid separation | | |
|---|---|---|---|
| | Isodose plan (%) | Bioeffect plan (%) | |
| $^{60}$Co beam | +25 | 34 × 2.0 Gy | +36 |
| 4 MV beam | +21 | 33 × 2.0 Gy | +32 |
| 10 MV beam | +16 | 31 × 2.0 Gy | +24 |
| 18 MV beam | +11 | 29 × 2.0 Gy | +16 |

It is not generally appreciated that such high effective doses are given anteriorly. It is not surprising that induration in the anterior axilla, arm edema, impaired shoulder mobility, and occasionally brachial plexpathy may occur as late effects, especially if combined with chemotherapy.

### *Chest Wall*

There are particular problems associated with treating the chest wall with opposed tangent fields. These include the change in surface contour with off-axis plans and the change in the volume of lung in the field at different levels. The definition of lung anatomy may be difficult and while a CT scan is preferable it may not be possible to scan patients in the treatment position.

The variations in dose and biological effect in the central, upper, and lower slices of the chest wall are examined below. Twenty-five fractions of 2.0 Gy per fraction were prescribed to the isocenter in the central slice using a 4 MV wedged beam, ssd = 105 cm. The bioeffect model and parameter values used were the same as those used for the axillary fields.

Figure 10.49 is a dose display in cGy in which lung corrections are included. The central slice plane shows 200 cGy at the isocenter, 212 cGy at the hot spot, and 205 cGy in the peripheral regions of the chest wall. This plan shows a reasonably uniform dose with the hot spot 3.4% higher than the peripheral dose. The biologically effective dose in the hot spot is the equivalent of 27 fractions compared with 25 fractions (+8%) at the isocenter and 26 fractions of 2.0 Gy at the peripheral region, as is shown in figure 10.50.

When the upper and lower slices are compared with the central slice, larger differences occur, especially in the lower slice, as shown in the bioeffect plan figure 10.51. Figure 10.51 shows that the hot spot receives the biological equivalent of 30 fractions of 200 cGy, 20% higher than the prescribed dose, at the isocenter. Isodose planning in this slice shows a smaller difference of 15%.

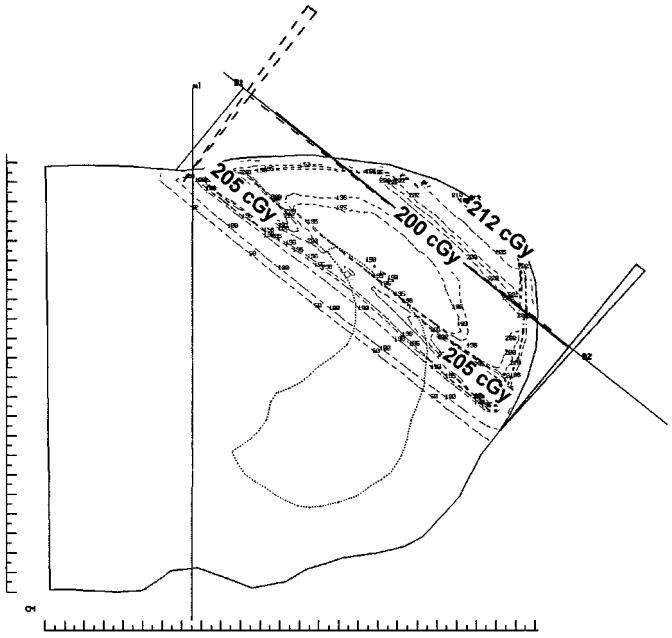


**Figure 10.49** A "rad display" plan of the central slice using lung corrections. Twenty-five fractions of 200 cGy at isocenter were delivered using a 4 MV beam.

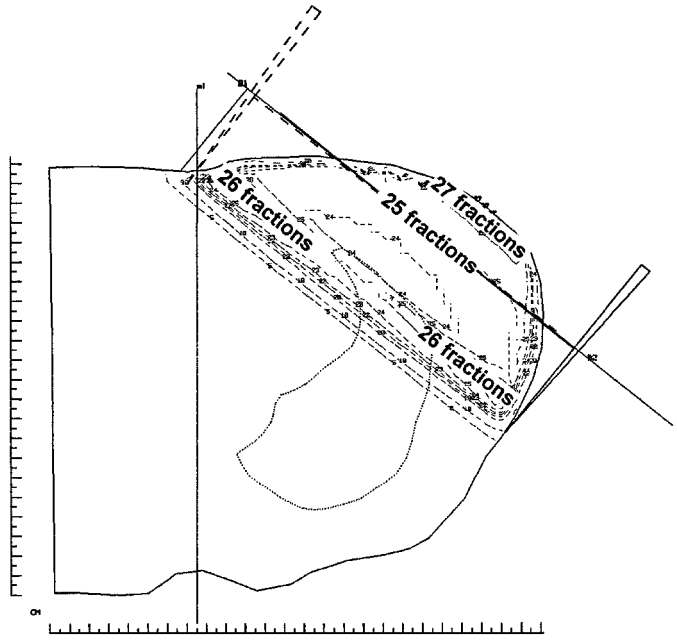


**Figure 10.50** A bioeffect plan of the central slice. Units of biological effect are described in terms of the number of fractions of 200 cGy per fraction.

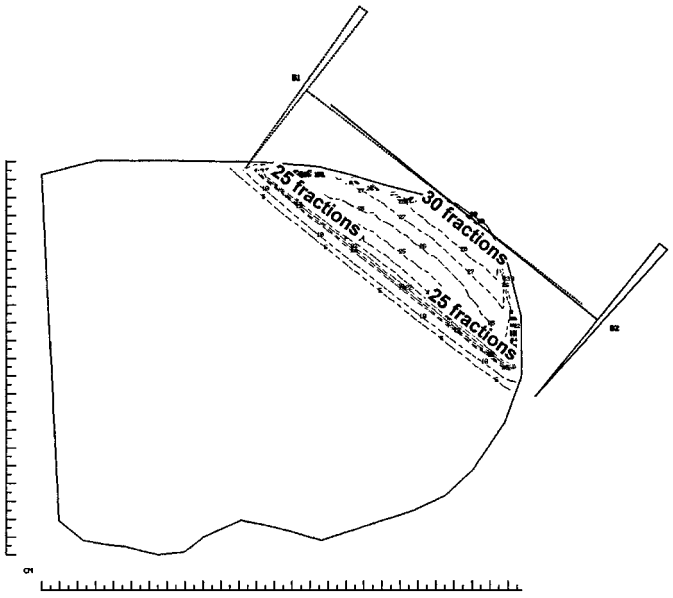


**Figure 10.51** A bioeffect plan on the lower slice for the same treatment as in figures 10.49 and 10.50.

**Table 10.6** The differences, expressed in percent, between predicted effects when comparing the hot spot regions with the peripheral dose regions in each slice, or the hot spot regions with the isocenter dose in the central slice when treating the chest wall. 4 MV beam, ssd = 105 cm.

| | Hot spot vs. peripheral dose region | | Hot spot vs. dose at isocenter of central slice | |
|---|---|---|---|---|
| Slice level | Isodose plan (%) | Bioeffect plan (%) | Isodose plan (%) | Bioeffect plan (%) |
| Central slice | +3.4 | +3.8 | +7.3 | +8.0 |
| Upper slice | +7.1 | +11.5 | +10.6 | +16.0 |
| Lower slice | +11.6 | +20.0 | +15.3 | +20.0 |

Comparison between isodose and bioeffect predictions at each slice are summarized in table 10.6. From this table it can be seen that, despite using wedged fields, a variation of up to +20% occurs and that isodose planning in each case underestimates the biological effect.

As shown in table 10.1, applied to parallel pairs of fields, beam quality influences the disparity between dose and effect. The disparities are greatest with $^{60}$Co beams and less using 18 MV beams compared with 4 MV beams. The magnitude of these differences depends on the separation values.

The breast technique always provides difficulties in planning. Treatment of the axilla presents particular problems, the magnitude of which are most clearly demonstrated by bioeffect planning. Tangential fields to the chest

wall also present particular problems associated with intervening lung in the fields and changing contours of the chest wall. In both cases isodose planning underestimates the inhomogeneity of biological effect compared with bioeffect planning. Bioeffect planning provides a means of quantifying the effective dose better than isodose planning and also a better means of planning to avoid regions of excessive dose.

### 10.5.8 Isodose, Bioeffect, and TCP Plans for a Case of Nonsmall Cell Carcinoma of the Lung: The Effects of Lung Density

The following example is a case with a large nonsmall cell carcinoma of the lung and mediastinum treated with AP-PA fields to near spinal cord tolerance and then boosted with a three field technique. A 6-MV beam, sad = 100 cm, 23 fractions of 2.0 Gy at the isocenter in the tumor was used. The tumor volume determined from CT images has been outlined in each of the figures 10.52–10.57.

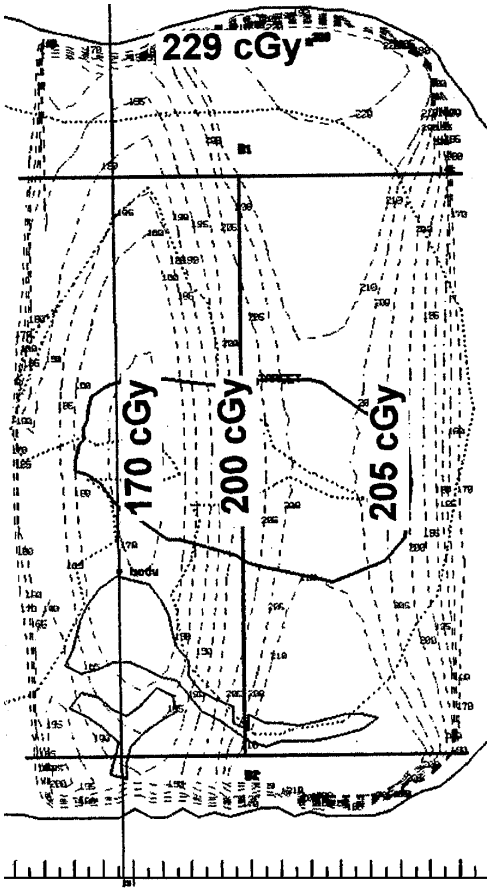


**Figure 10.52** The dose per fraction distribution with a 6 MV beam when 200 cGy is prescribed at the isocenter and lung corrections have been included.

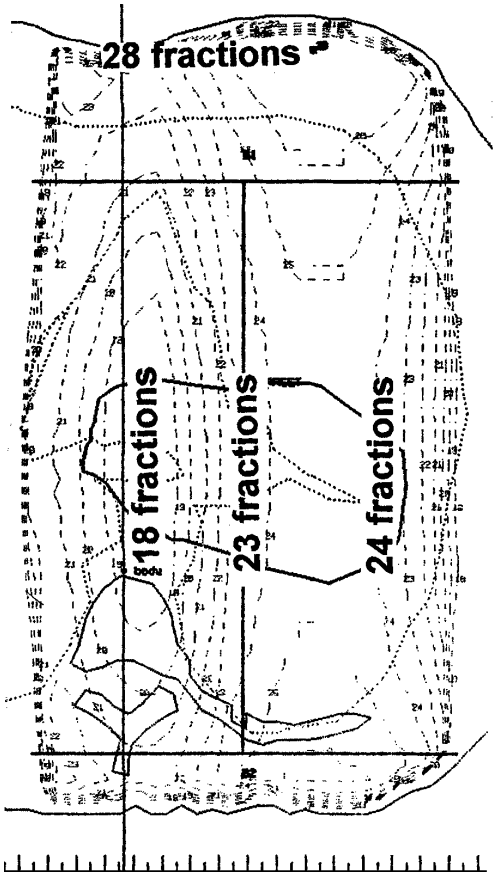


**Figure 10.53** A bioeffect plan of figure 10.52 in which 23 fractions are prescribed. The biologically effective dose to normal tissue is described as the equivalent number of fractions of 200 cGy. Lung corrections have been included.

Figure 10.52 is a lung corrected dose display showing 200 cGy per fraction at isocenter and 229 cGy in the peak region. Because of the effect of intervening lung the dose per fraction varies between 170 and 205 cGy within the tumor volume. The same plan without lung correction results in a practically uniform dose per fraction of 200 cGy in the tumor volume and a peak dose of 252 cGy.

Lung correction is necessary to demonstrate the variability of the dose per fraction in the spinal cord. At the tumor isocenter 200 cGy was prescribed but the cord dose in the treated volume from the sternal notch to 4 cm inferior to the isocenter varied from 180 to 160 cGy. Without lung correction the dose varied between 200 and 226 cGy per fraction. In the tumor region the 3-field technique added seven fractions of 125 cGy to the spinal cord. Summation of partial treatments, for example, using look-up

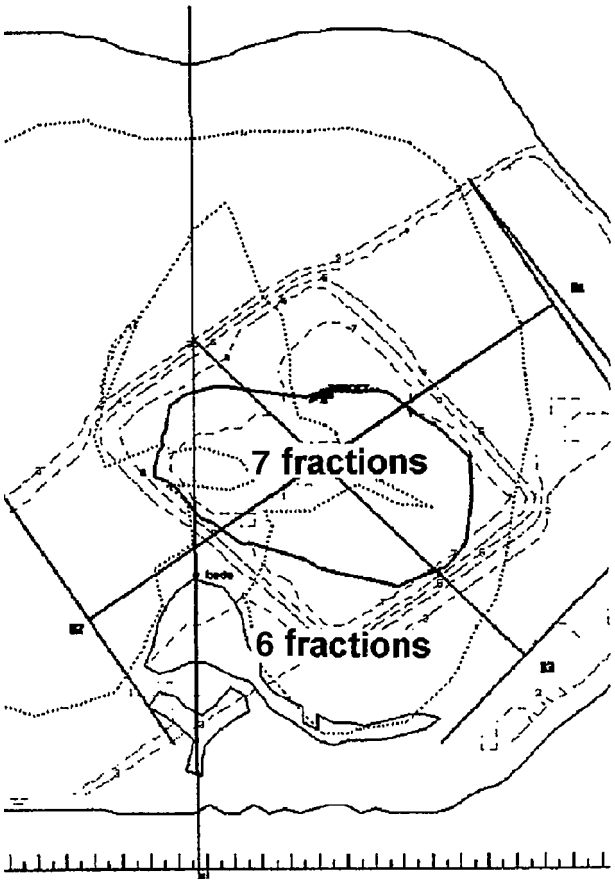


**Figure 10.54** A bioeffect plan of seven fractions of 200 cGy at the isocenter.

graphs or the equation shown in figure 1.10, with an $\alpha/\beta = 2.0$ Gy for spinal cord the biologically effective dose in the cord varied from 20.1 to 24.8 fractions of 2.0 Gy equivalence. Clearly, the variation in patient anatomy from region to region and particularly the intervening lung significantly affects the biologically effective cord dose, and this is not readily appreciated with simple percent isodose plans, especially if uncorrected for lung density. Bioeffect planning also permits summation of partial treatments either by the use of "look-up" graphs or by a full bioeffect plan for spinal cord.

Figure 10.53 is a bioeffect plan of figure 10.52 applied to late-reacting normal tissues. As shown in table 8.7, an $\alpha/\beta$ value of 3.0 Gy is an appropriate value to use for late fibrosis, as may apply to mediastinal structures and late lung fibrosis. The model used was equation (1.19) with $\alpha/\beta = 3.0$ Gy, $\phi = 0.081$, $d_s = 2.0$ Gy, the target and reference volumes were assumed to be identical $10 \times 10 \times 10$ cm. At the peak region the effective

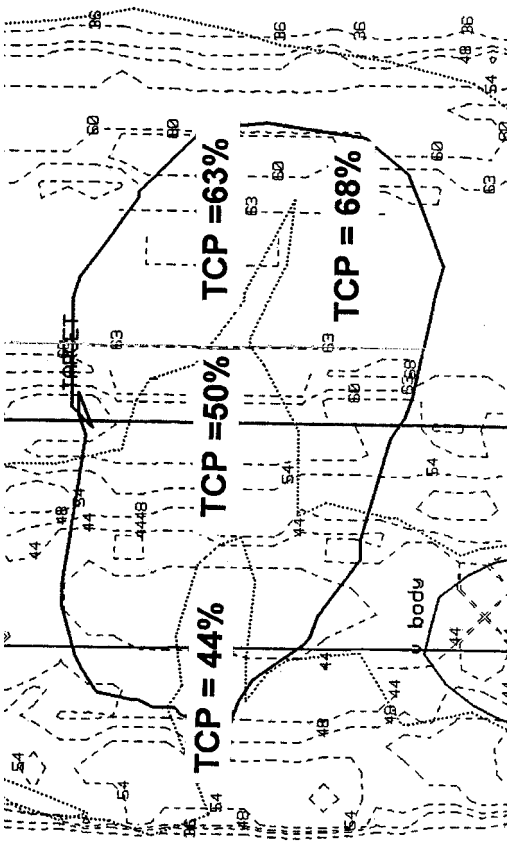


**Figure 10.55** Predicted percent tumor control probabilities in which inhomogeneities of parameter values are included, as occur in populations of patients. The figures only apply to the tumor region outlined.

dose is the equivalent of 28 fractions of 200 cGy, while in the tumor volume the biologically effective dose varies between 18 and 24 fractions of 200 cGy. A bioeffect plan uncorrected for lung density shows only a small variation of effective dose in the tumor volume between 23 and 24 fractions of 200 cGy, although at the peak region the effective dose is $32 \times$ 200 cGy. Figure 10.54 is a lung corrected bioeffect plan of the 3-field technique using seven fractions of 200 cGy at the isocenter. This shows that the variation of the biologically effective dose in late-reacting tissues in the tumor region lies between six and seven fractions.

As shown in figure 10.52, there is a substantial variation in dose per fraction in the tumor volume due to the intervening lung. The effect of this on TCP is shown in figure 10.55. Equation (9.9) in the EFFECT model described in chapter 9 has been used to produce TCP estimates assuming a uniform clonogen cell density. The parameter values were $\alpha_m = 0.38$, $\alpha_\sigma = 0.088\ \text{Gy}^{-1}$, $\beta_m = 0.042$, $\beta_\sigma = 0.029\ \text{Gy}^{-2}$, $T_{pm} = 4.7$, $T_{p\sigma} = 3.2$,

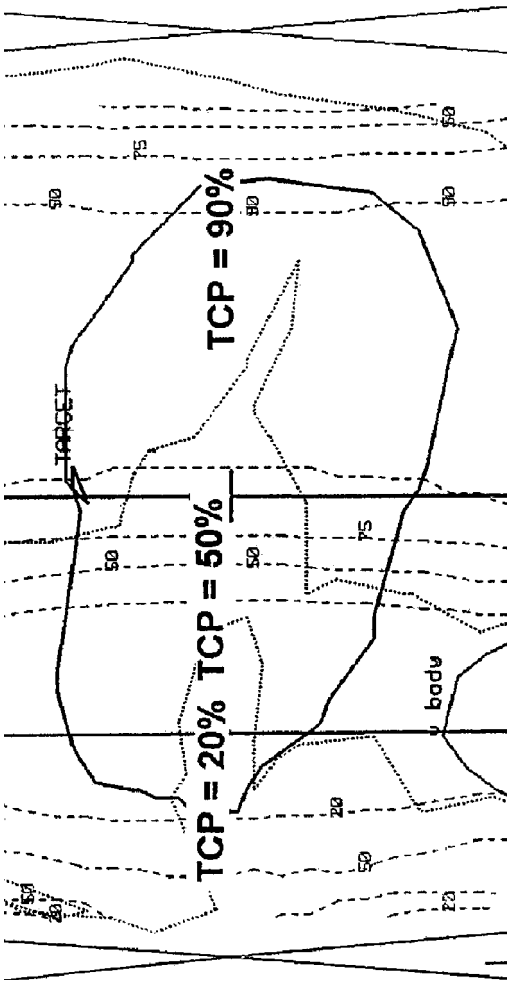


**Figure 10.56** Predicted percent tumor control probabilities in which only the mean parameter values are used. The steeper TCP curves are reflected in a larger variation in TCP than in figure 10.55. The figures outside the tumor volume are meaningless.

$T_o = 46.2$, $T_s = 0$, $T_k = 7$ days, $d_{g\sigma} = 0.05$ Gy, $h_{mt} = 0$. The clonogen numbers were adjusted to give a 50% TCP near the center of the tumor, therefore $M_m = 10^4 \times 3.5^3$. Figure 10.55 shows that as a consequence of the variation of fraction size the predicted TCP varied between 44% and 68%.

As was described in chapter 9, TCP predictions, which include inhomogeneity corrections, as used above, are more likely to approximate clinical realities for populations than a simpler model in which only mean parameter values are used, in which case predicted TCP curves are much steeper and more sensitive to changes in dose per fraction. Equation (9.42) shown in the CONFRACT model describes TCP using mean parameter values only. In this model fractionated and brachytherapy

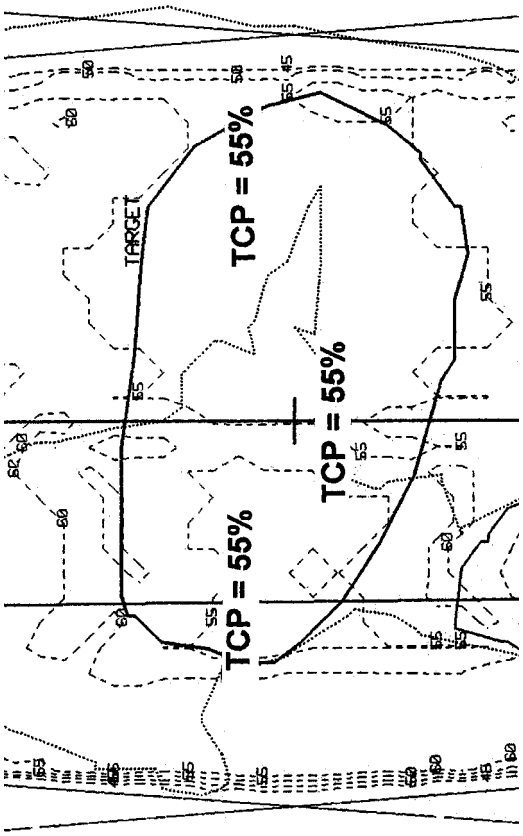


**Figure 10.57** The same treatment and same model has been used, as in figure 10.56. In this example a tissue compensator has been used. The TCP is now uniform throughout the tumor volume outlined.

treatments may be considered alone or combined. In figure 10.56, TCP calculations for fractionated treatment have been made using this model for 23 daily fractions of 2.0 Gy at the isocenter, as used in figure 10.52. The values used were $N = 23$, $\alpha_m = 0.38\ \text{Gy}^{-1}$, $\beta_m = 0.042\ \text{Gy}^{-2}$, $T_{pm} = 4.7$ days, $nd = 1$, $h_{mc} = 0$, and as no brachytherapy was used $R_a = 0$ and $tm = 0$. The clonogen number $M_m$ was adjusted to $2.6 \times 10^6$, so a TCP of 50% occurs in the same position within the tumor as in figure 10.50 thereby permitting comparisons.

Comparison of figures 10.55 and 10.56 show that there is a much bigger variation in predicted TCP rates in figure 10.56 with values 20–90% compared with 44–68% when inhomogeneities of parameter values are included. Even with the more conservative TCP estimates bioeffect planning shows a large variation in TCP rates as a consequence of the effect of intervening lung. Although not shown, the extra variation in TCP within the 3-field technique was small as the dose was nearly homogeneous.

Isotumor control probability planning is the logical aim of optimum treatment. The above examples show clearly that, assuming a uniform clonogen cell density, a very large variation in TCP occurs. Although rarely done, a tissue compensator may be used to produce a uniform dose per fraction and TCP within the tumor volume, as shown in figure 10.57. The model and treatment used in figure 10.57 was identical to that used in figure 10.55 except that the clonogen numbers where adjusted to give a 55% TCP at the isocenter.

The actual TCP values shown are only approximations but are particularly useful to show the variability of the effect as a consequence of variation of fraction size within the tumor volume. Clearly, isodose plans without lung corrections would give a poor indication of potential variability of TCP. Lung corrected dose per fraction displays more clearly indicate that substantial variations in TCP are likely. Bioeffect TCP plans clearly describe the potential magnitude of TCP variability. The variability of biologically effective dose on the spinal cord should also be noted. In the examples shown alternate plans should be made to reduce the TCP "cold" spots. Although not developed yet in this system, it is conceivable that TCP bioeffect plans may be used to design compensators to generate iso-TCP plans, which are generally the aim of treatment with curative intent.

### 10.5.9 Summation of Fractionated and Continuous Irradiation

#### *Low Dose Rate Brachytherapy and Effect on Dose-Limiting Late-Reacting Tissues*

In chapter 3 a model was derived for the summation of fractionated daily treatments or hyperfractionated treatments with continuous irradiation. The method was described by equation (3.26) and is demonstrated in figures 3.21 and 10.67. In the following examples of treatment of a case of carcinoma of the cervix 12 daily fractions of 2.0 Gy per fraction were given to a pelvic field using a 4 MV beam. A course of brachytherapy was planned using a 6-cm line of $^{137}$Cs pellets within the uterus and sources within the vaginal vault to deliver 50.0 Gy at Point A. Two dose rates at Point A were examined at 0.4 and 1.0 Gy $h^{-1}$.

Figure 10.58 is a "rad display" showing the total dose given with the external beam. Figure 10.59 is a rad display of the brachytherapy showing 50.0 cGy delivered at Point A. Figure 10.60 is also a rad display and shows the sum of the fractionated and continuous treatment with 74.0 Gy at Point A and also shows the isodose contour for a total dose of combined treatment at the 40.0 Gy contour.

Figures 10.61 and 10.62 are bioeffect plans using equation (3.26) at two different dose rates of 0.4 and 1.0 Gy $h^{-1}$. The biological effect is expressed

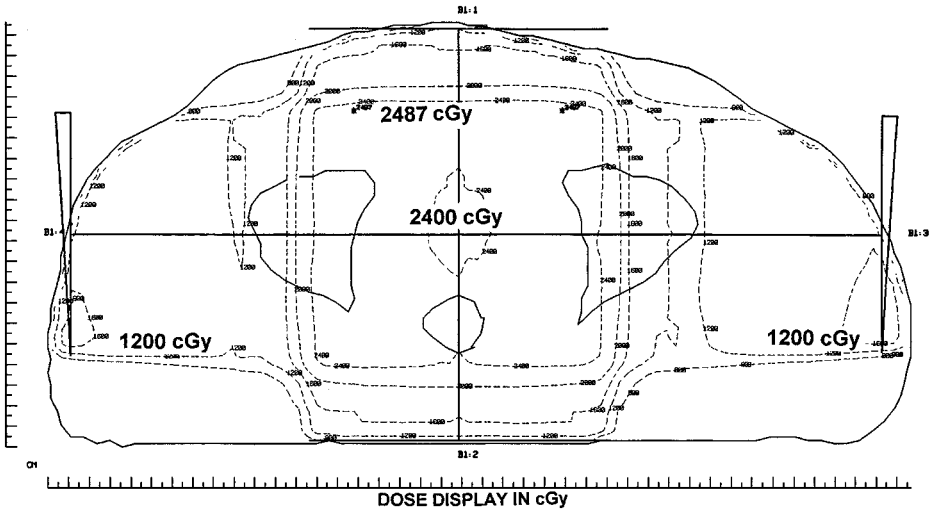


**Figure 10.58** Isodose plans showing the total dose in rad (cGy). Figure 10.58 shows the dose distribution of 12 fractions of 2.0 Gy.

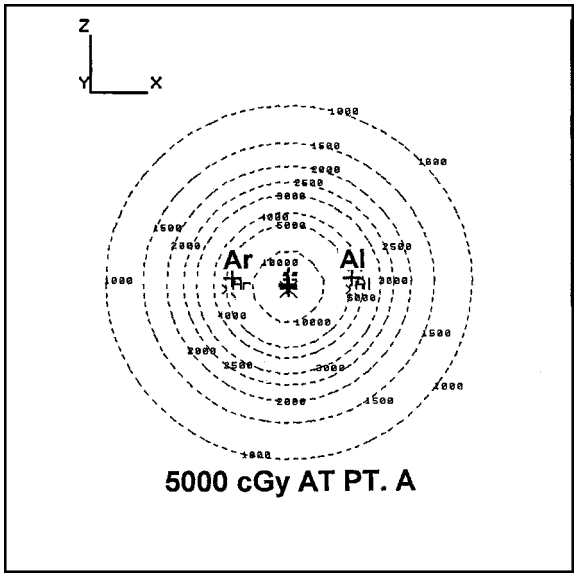


**Figure 10.59** Isodose plans showing the total dose in rad (cGy). Figure 10.59 shows the total dose from a brachytherapy source prescribed to 50.0 Gy at Point A.

as the equivalent of 2.0 Gy fractions to late-reacting tissue with $\alpha/\beta$ value of 3.0 Gy and a repair constant $\mu = 0.46\ h^{-1}$.

As would be expected from chapter 3, the isodose plan and the bioeffect plan, when the brachytherapy was given at 0.4 Gy $h^{-1}$, are almost identical. The isodose and bioeffect lines for the total dose of 70.0 Gy equivalent

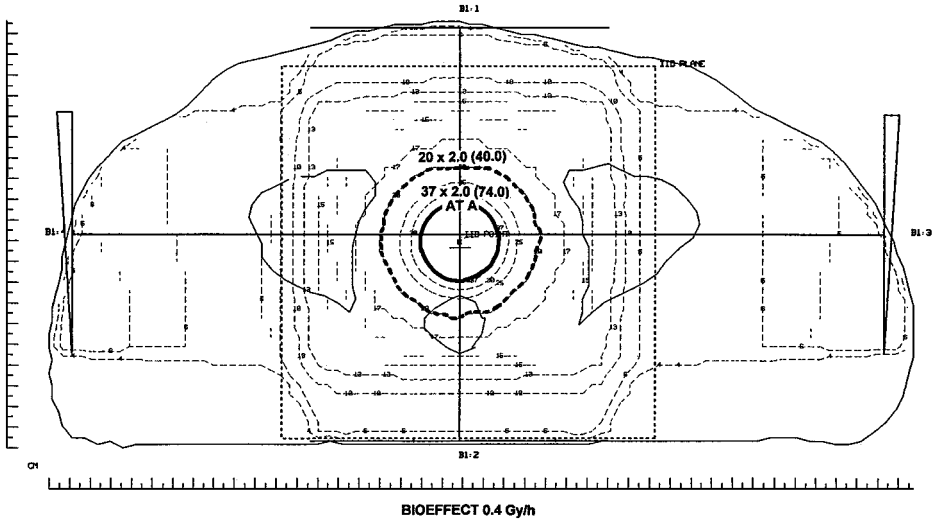


**Figure 10.60** Isodose plans showing the total dose in rad (cGy). Figure 10.60 shows the combined total dose of 37 × 2.0 Gy at Point A (highlighted continuous line) and also at the 40.0 Gy isodose line (dotted line).

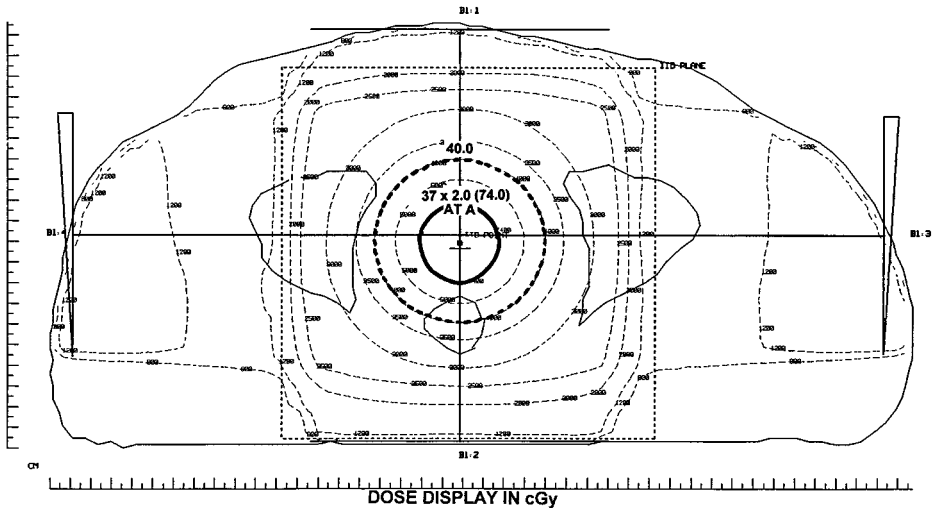


**Figure 10.61** The biologically effective dose in units of 2.0 Gy per fraction from combined treatments using a dose rate of continuous irradiation of 0.4 Gy $h^{-1}$. The highlighted continuous lines in both figures 10.61 and 10.62 are the isoeffect contours of 37 × 2.0 Gy equivalent dose which may be compared with the isodose plans shown in figure 10.60.

pass through Point A. When the dose rate was increased to 1.0 Gy $h^{-1}$ as shown in figure 10.62, the 74.0 Gy equivalent isoeffect line expanded compared with the same equivalent isoeffect line at the lower dose rate as shown in figure 10.61. The volume encompassed by a 6-cm cylinder

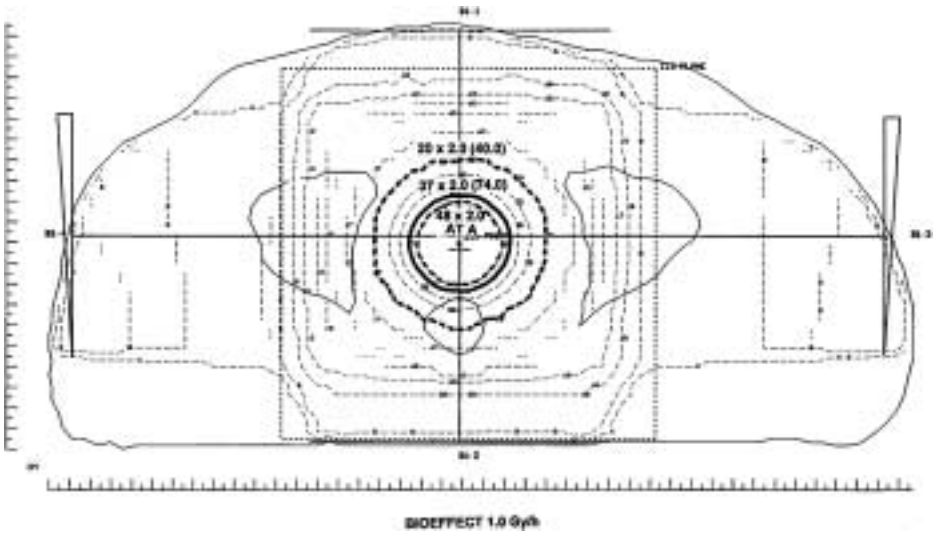

**Figure 10.62** The effect of increasing the dose rate of brachytherapy to 1.0 Gy $h^{-1}$.

and the 74.0 Gy bioeffect line for the higher dose rate technique is approximately 117 mL compared with 72 mL for treatment using 0.4 Gy $h^{-1}$. This represents a 63% increase in volume with the consequent tolerance implication. At Point A the biological equivalent of the higher dose rate is $48 \times 2.0$ Gy compared with $37 \times 2.0$ Gy at the lower dose rate. Clearly, the dose rate effect as shown in these examples will have a significant effect on both tolerance and TCP.

The dose rate effect demonstrated in these examples is not only a consequence of the fall of dose with distance but also is compounded by the decreasing biological effect as the dose rate falls. This effect is very similar to the disparities between dose and effect with fractionated treatment. It is very difficult to appreciate in three dimensions the biologically effective dose as it changes with physical dose and dose rate without bioeffect planning.

The same principles applied to changes in TCP with steeper gradients of TCP curves occurring at the margin of the target volume than would be anticipated when considering the physical dose only.

A particular application of this model is the facility to adjust the ratios of external beam treatment and intracavity treatment or to adjust the loading of the external beam treatment to more nearly conform to the tumor volume, as shown in figures 10.63 and 10.64.

Figure 10.63 shows the biologically effective dose in terms of 2.0 Gy fractions using the same method as in figures 10.61 and 10.62 but treating a different patient, and no external beam treatment has been used.


**(A)**

**Figure 10.63** The bioeffect contours in units of 2.0 Gy fractions using a dose rate of 1.0 Gy $h^{-1}$ at 2.0 cm from the center. Reading from the center outwards the bioeffect contours are 100, 50, 25, 20, 15, 10, and 5 fractions of 2.0 Gy. The arrow indicates the 25 fraction contours. No external beam radiotherapy has been used. Figures (A) and (B) are the same plans using differing contrast to help demonstrate the contours more clearly.

A single line source of $^{137}$Cs seeds was used to deliver 50.0 Gy at 2.0 cm at 1.0 Gy $h^{-1}$. The bioeffect contours are symmetrical about the center. This may not be suitable if there is any risk of spread laterally into the parametrium. Equation (3.26) permits the summation of external beam treatments and this application is shown in figure 10.64, in which a right lateral 23 MV beam has been used to boost the right parametrial biological dose to a satisfactory level. The interactive planning system permits

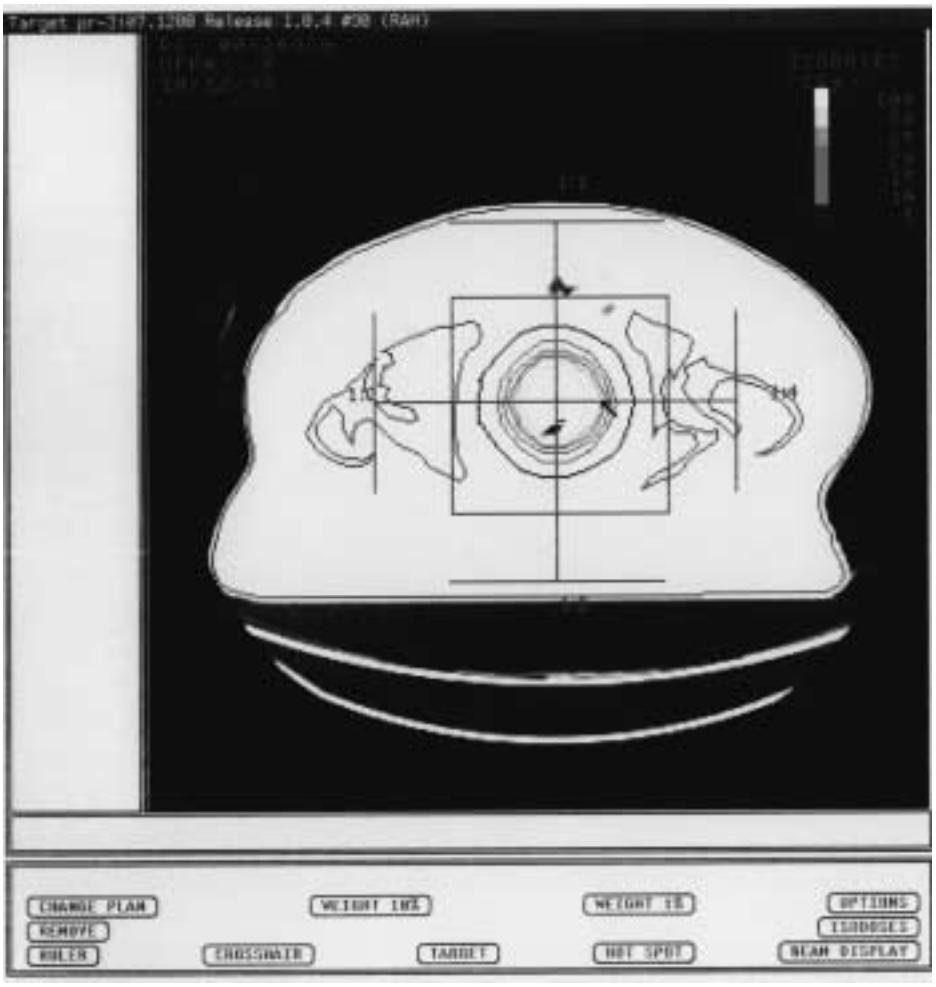


**(B)**

**Figure 10.63** (Continued.)

the choice of the preferred plan; for example in figure 6.64, 25 fractions of 2.0 Gy at $d_{max}$ have been used.

Figure 10.63 shows the fall in the biologically effective dose with distance from the intracavity line sources when a dose rate of 1.0 Gy $h^{-1}$ is given at 2.0 cm. As the distance increases, the fall in biologically effective dose with distance is dependent on the inverse square law, attenuation, and also with change in dose rate. If a higher dose rate is used, the biologically effective dose at distance will be greater than with low dose rates. Figure 10.65 shows how the biologically effective dose at distance from the sources increases when dose rate varies between 0.5 and 150.0 Gy $h^{-1}$. These curves were derived from a series of bioeffect plans similar to figure 10.63 but with differing dose rates. The curves are not perfectly


**(A)**

**Figure 10.64** The same as figure 10.63 except 25 fractions of 2.0 Gy have been added with a 23 MV beam. The bioeffect contours have the same values as in figure 10.63 but have expanded and skewed towards the right parametrium. The arrow indicates the 25 fraction contour which is now displaced to the right as required. Figures (A) and (B) are the same plans using differing contrast to help demonstrate the contours more clearly.

smooth as the data were derived by measuring the rather thick and irregular contour lines produced by the planning system. Also shown in figure 10.65 is the physical dose derived from an isodose plan using a rad display.

Figure 10.65 shows that the isodose and bioeffect curves are similar at low dose rates. For example, a total dose of 50.0 Gy occurs at 2.0 cm and 50.0 Gy (in 2.0 Gy fractions) at 2.3 cm from the sources. As the dose rate increases, the distance at which 50.0 Gy in 2.0 Gy fractions occurs

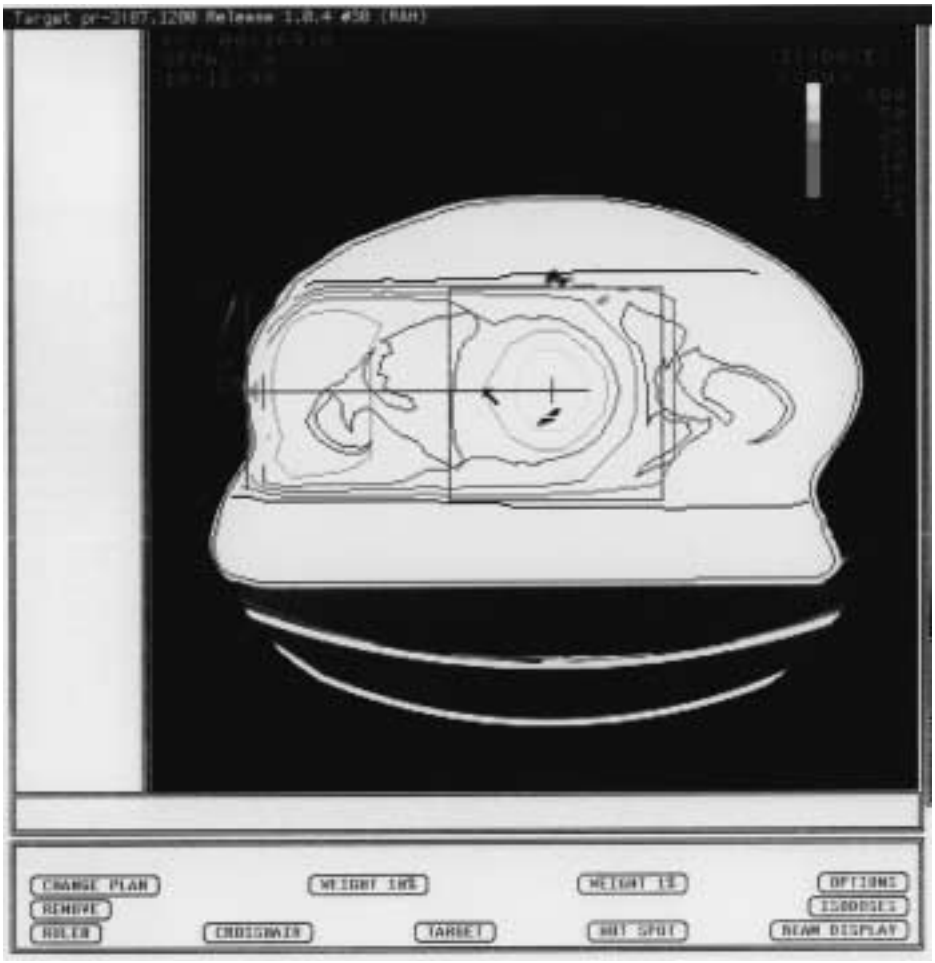


**(B)**

**Figure 10.64** (Continued.)

increases to 3.9 cm at 150 Gy $h^{-1}$. The change in the dose rate effect is greatest at low dose rates of 10.0 Gy $h^{-1}$ or less. With higher dose rates there is much less sensitivity to changes in the dose rate, as shown in figure 10.67.

Figure 10.66 shows the effect of adding 12 fractions of 2.0 Gy per fraction to the same brachytherapy treatment, as shown in figure 10.65. The effect is to force the bioeffect curves away from the sources. This is most marked as the distance increases and the brachytherapy and dose rate effect wanes compared with the contribution from the fractionated treatment. The bend in the curves at approximately 5.0 cm from the sources is at the beam edge of the AP-PA fields.

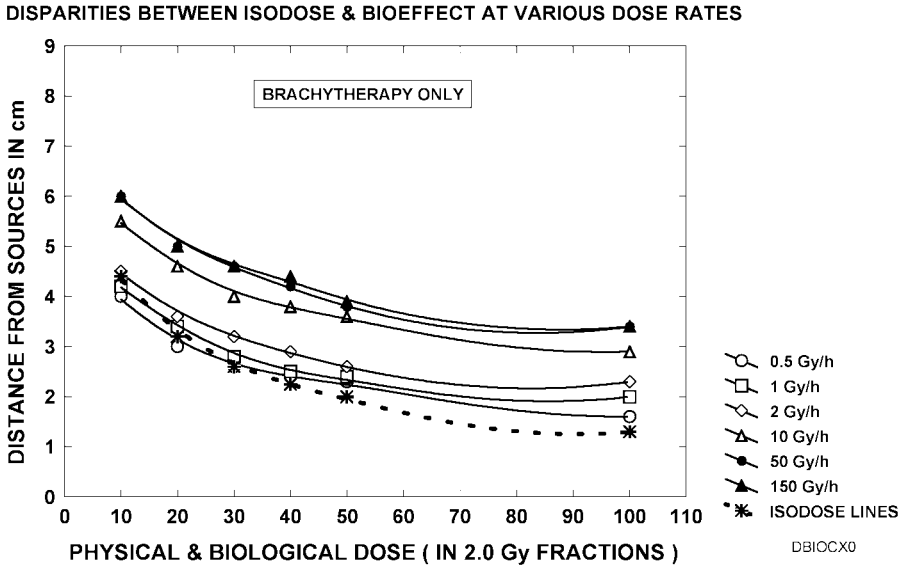


**Figure 10.65** Differences between isodose and bioeffect curves with distance from the sources as the brachytherapy dose rates are varied between 0.5 and 150.0 Gy $h^{-1}$.

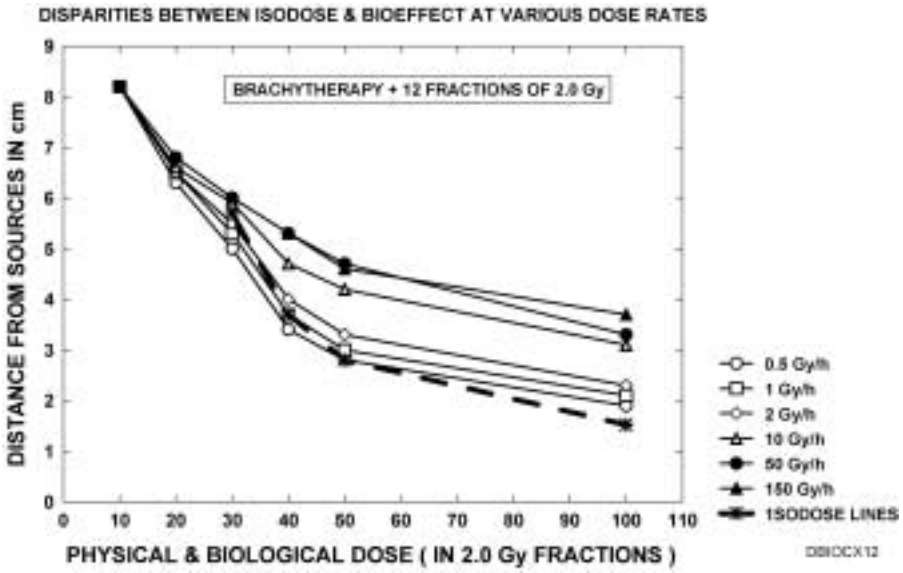


**Figure 10.66** As in figure 10.65 but 12 fractions of 2.0 Gy external beam treatment are also given.

The sensitivity of the biologically effective dose to dose rate changes is shown in figure 10.67. This shows a diminishing sensitivity to dose rate effects as the dose rate increases. This figure was derived by plotting the dose of continuous irradiation on the vertical axis against the

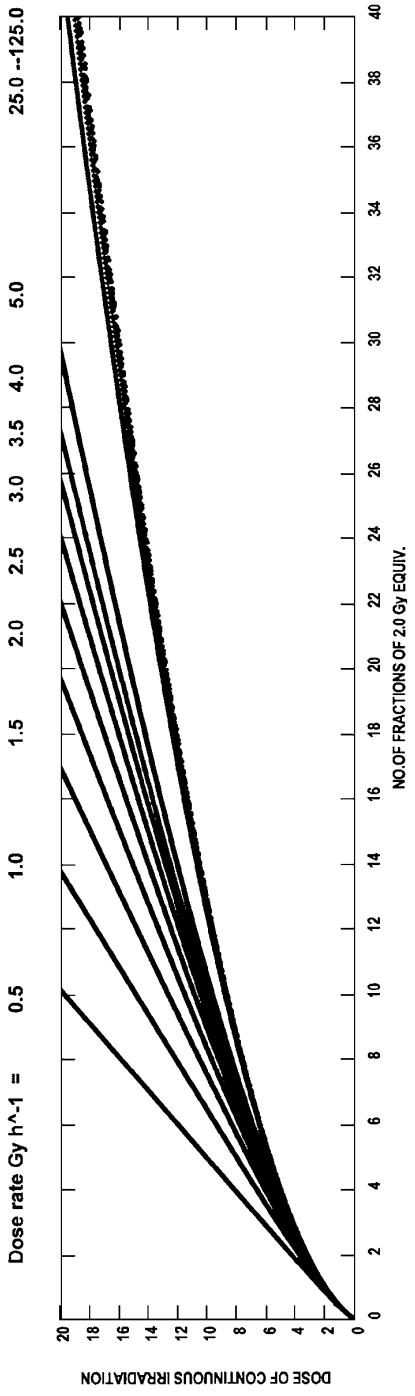


**Figure 10.67** The sensitivity of the biological effect to change in dose rate is highest with low dose rates. There is little difference between 25.0 and 125.0 Gy $h^{-1}$.


**(A)**

**Figure 10.68** A bioeffect plan, the contours of which are in units of number of fractions of 2.0 Gy. Twenty-five fractions of 2.0 Gy are combined with 10.0 Gy given at 1.0 cm at 150.0 Gy $h^{-1}$. Figures (A) and (B) are the same plans using differing contrast to help demonstrate the contours more clearly.

biologically effective dose in 2.0 Gy fractions described by equation (3.26) on the horizontal axis. This is the same method as used in figure 3.21. Clearly, it is important to include dose rate effects in any brachytherapy plans.

### *High Dose Rate Brachytherapy (HDR) and the Effect on Dose-Limiting Late-Reacting Tissues*

Figure 10.68 is an example of combined high dose rate brachytherapy and fractionated external beam treatment as in the treatment of carcinoma of the esophagus. In this example 25 fractions of 2.0 Gy were

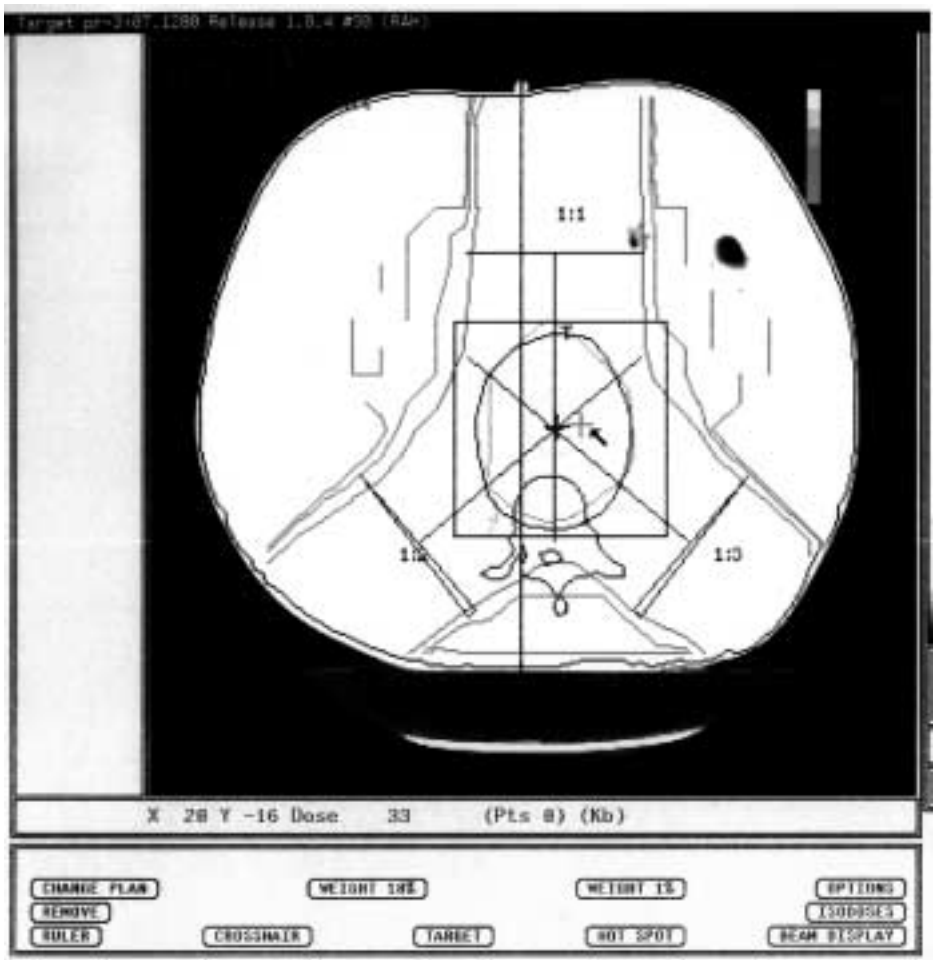


**(B)**

**Figure 10.68** (Continued.)

prescribed at the isocenter using a 3-field technique, together with 10.0 Gy of continuous irradiation prescribed at 1.0 cm at 150.0 Gy $h^{-1}$. A $^{192}$Iridium source with an active length of 5.0 cm was used.

Figure 10.68 shows the summated biologically effective dose expressed as the number of fractions of 2.0 Gy. The disparities between the effects predicted by isodose plans and bioeffect plans are shown in figure 10.69. For example, at 1.0 cm distance the isodose plot shows a total dose of 60.0 Gy at 1.0 cm, whereas the biologically effective dose is 82.0 Gy at 2.0 Gy per fraction. As before the bioeffect curves are not smooth due to inaccuracies measuring the rather irregular contours produced by the planning system.

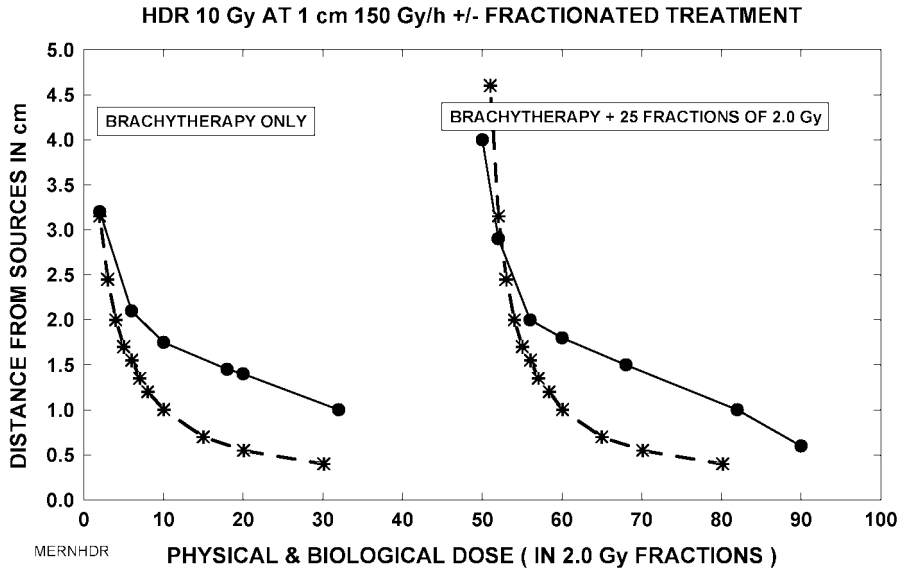


**Figure 10.69** Differences between effect predicted by isodose plans and bioeffect plans when HDR brachytherapy of 10.0 Gy at 150.0 Gy $h^{-1}$ at 1 cm is given alone or combined with 25 fractions of 2.0 Gy.The broken lines are the total dose and the continuous lines are the biologically effective dose at 2.0 Gy per fraction.The differences are due to the dose rate effects.

The disparities decrease with distance as the dose rate and dose rate effect decreases. Figure 10.69 also shows the same effect with brachytherapy alone, although the curve shifts to the left. Clearly, the dose rate effect has a profound influence on the biologically effective dose. Isodose and bioeffect curves would be identical if there was no dose rate effect.

## 10.6 Published Papers by the Author on Bioeffect Planning

Published papers on bioeffect planning are shown in Appendixes A, B, and C. In addition, figures 10.4 and 10.5 are from Wigg (1985), and the cases shown in figures 10.7–10.15 are from Kwitko et al. (1982). The paper in Appendix A was presented at the Second International Conference on Dose, Time, and Fractionation in Radiation Oncology, Madison, Wisconsin, September 1984. Appendix B was presented by Nicholls at the Eighth International Conference on The Use of Computers in Radiation Therapy, July 1984. In this paper the early software modifications by Nicholls of the IGE Planning System are described. Subsequently, further modifications have been made to the IGE Target

Planning System and more models have been included and these are shown in Appendix C.

The biological consequences of treating one field per day were described by Wigg and Wilson (1981) and this was the stimulus to proceed to the ultimate development of the Adelaide Bioeffect Planning System

# SHADES OF GRAY

THE OTHER DAY I MET A GRAY
AND WONDERED WHAT HE HAD TO SAY
WHAT HE WAS AND WHAT HE DID
AND ANY SUBTLETIES HE HID.

ONE JOULE PER KILO HE SAID TO ME
THERE IS NOTHING HIDDEN AS YOU CAN SEE.
NO MORE NO LESS CAN BE HAD
BEING A CLONE OF MY DAD THE RAD.

BUT HOW IS IT SO THAT THE EFFECTS I SEE
ARE NOT SO PRECISE AS YOU CLAIM TO BE?
SURELY IT IS YOUR EFFECT ON TISSUE
THAT IS THE FUNDAMENTAL ISSUE.

THAT'S TRUE HE SAID. A DILEMMA I SEE
THAT I AM SO PRECISE BUT SEEM NOT TO BE.
DEEPER AND DEEPER WE DEBATED THE ISSUE
OF THE ABSORPTION IN MATTER AND EFFECTS ON TISSUE.

A COMPLETE AGREEMENT COULD NOT BE FOUND
THOUGH THE ARGUMENTS PUT WERE CONCEPTUALLY SOUND
ALTHOUGH NOT TRUE WE AGREED TO SAY
IT HELPS TO THINK IN SHADES OF GRAY.

SHADES OF GRAY, SHADES OF GRAY
WHAT A FUNNY THING TO SAY!

D.R.W.